Palaeogeography, Palaeoclimatology, Palaeoecology 603 (2022) 111208

Contents lists available at ScienceDirect

Palaeogeography, Palaeoclimatology, Palaeoecology

journal homepage: www.elsevier.com/locate/palaeo

Negative $\delta^{13}C_{carb}$ values at the Jurassic-Cretaceous boundary – Vaca Muerta Formation, Neuquén Basin, Argentina

Leticia Rodriguez Blanco [a,b,*], Peter K. Swart [b], Gregor P. Eberli [b], Ralf J. Weger [b]

[a] Department of Geosciences, University of Oslo, Oslo, Norway
[b] CSL – Center for Carbonate Research, University of Miami, Miami, USA

ARTICLE INFO

Editor: S Xie

Keywords:
Diagenesis
Anoxia
Shale
Vaca Muerta
Carbonate isotope

ABSTRACT

The stable carbon isotopic compositions of carbonate sediments ($\delta^{13}C_{carb}$) have been widely used to reconstruct the global carbon cycle and as a stratigraphic correlation tool. This work investigates a $\delta^{13}C_{carb}$ record of marine organic-rich, mixed siliciclastic-carbonate mudstones accumulated from the Tithonian (late Jurassic) to the early Valanginian (early Cretaceous) in a retro-arc basin connected to the Proto-Pacific Ocean (Neuquén Basin, Argentina). The high-resolution record of $\delta^{13}C_{carb}$ values of these strata from outcrops at various locations in the basin differ from those in the coeval pelagic strata of the Tethys. The $\delta^{13}C_{carb}$ profile in the Puerta Curaco area shows an overall increasing trend from average values of −7‰ (early Tithonian) to approximately 0‰ (early Valanginian). The negative $\delta^{13}C_{carb}$ values occur in a ~ 400 m thick TOC-rich succession (TOC > 2%) and are arranged in 3 large-scale increasing-decreasing cycles. Although absolute values are offset, main trends are similar in other outcrops and in subsurface wells. The co-occurrence of the highest U/Th (>1.4) and the most negative $\delta^{13}C_{carb}$ values suggests that the major trends in the $\delta^{13}C_{carb}$ profile might be modulated by oscillations in oxygen content within the basin probably driven by sea-level changes. Clastic-dominated transgressive hemicycles have higher TOC and more negative $\delta^{13}C_{carb}$ values while the opposite occurs in carbonate-rich regressive hemicycles. A trend from "normal" Tithonian surface-water values (avg. +2‰) in the southern shelf to increasingly negative $\delta^{13}C_{carb}$ values towards the basin center indicates a mixing between platform-derived carbonate material unaffected by diagenesis and carbonate precipitated or altered in a dysoxic/anoxic basin. The $\delta^{13}C_{carb}$ profile in the Tethyan realm does not record this episode of high burial of organic carbon occurred in the Neuquén basin during the Tithonian and Berriasian but display a slightly decreasing trend between +2.5 and +1.5‰.

1. Introduction

The potential of marine carbonate isotope stratigraphy relies on the fact that $^{13}C/^{12}C$ ratios of marine carbonates have varied over time, mainly as the result of partitioning of carbon between organic carbon and carbonate carbon reservoirs in the lithosphere (Veizer et al., 1980; Kump and Arthur, 1999). While other factors such as diagenesis and sediment source are known to affect $\delta^{13}C_{carb}$ values, their primary use in the carbonate record has been in the interpretation of the isotopic composition of the oceans, which provide insight into global carbon cycle dynamics and can be applied as stratigraphic correlation tools (Saltzman and Thomas, 2012; Cramer and Jarvis, 2020). The formation of calcium carbonate and its burial in marine sediments accounts for approximately 80% of the total carbon removed from the Earth's surface, from which at least 10% would be due to authigenic carbonate precipitation (Sun and Turchyn, 2014). This proportion might be larger in the margins of ocean basins with high primary productivity and high delivery of organic carbon to marine sediments, as well as during times of oxygen deficiency (Schrag et al., 2013).

This work presents a case study from the Neuquén Basin, Argentina, where a high-resolution record of $\delta^{13}C_{carb}$ values has been measured through the Tithonian (late Jurassic)-early Valanginian (early Cretaceous) marine successions of the Vaca Muerta Formation. The original goal was to produce a $\delta^{13}C_{carb}$ profile of this time interval in an ocean basin on the southern hemisphere. We will, however, show how local burial of organic carbon and associated diagenesis result in $\delta^{13}C_{carb}$

* Corresponding author at: Department of Geosciences, University of Oslo, Oslo, Norway.
E-mail addresses: l.rodriguezblanco@geo.uio.no (L. Rodriguez Blanco), pswart@rsmas.miami.edu (P.K. Swart), geberli@rsmas.miami.edu (G.P. Eberli), rweger@rsmas.miami.edu (R.J. Weger).

https://doi.org/10.1016/j.palaeo.2022.111208
Received 10 November 2021; Received in revised form 15 August 2022; Accepted 17 August 2022
Available online 20 August 2022

trends that are not reflecting the global carbon cycle. The aims of the present work are: (a) to compare the Neuquén basin $\delta^{13}C_{carb}$ profile with that of the Tethyan region (typically considered representative of a "global signal"; Cramer and Jarvis, 2020); (b) to delineate the diagenetic processes that influence the $\delta^{13}C_{carb}$ profile; and (c) to explain the co-occurrence of highly negative $\delta^{13}C_{carb}$ values in the basin with "normal" Tithonian-Berriasian values on the shelf.

2. Geological setting

2.1. The Neuquén Basin

The Neuquén Basin lies within the eastern side of the Andean Cordillera, in west-central Argentina, between 32 and 40° south, and 71° and 68° west (Fig. 1A). During the late Jurassic and early Cretaceous, the area was part of the western Gondwana and evolved as a continental margin with active subduction of the proto-Pacific plate (Fig. 1B). The magmatic arc developed during this period was poorly evolved, the continental crust was attenuated and very close to sea level, and extensional basins such as the Neuquén Basin developed in the retro-arc (Uliana et al., 1995; Ramos and Aleman, 2000; Ramos, 2010). These retro-arc basins coincided with previous rift systems and were mainly controlled by thermal sag subsidence (Legarreta and Uliana, 1991; Franzese and Spalletti, 2001; Howell et al., 2005). As a result of this dominant extensional regime during Late Jurassic times, most of the continental margin of Gondwana was flooded by marine transgressions at the beginning of the Tithonian (Ramos et al., 2020). The Neuquén Basin contains a rich and diverse fossiliferous assemblage indicative of open marine waters that are similar to the forms in the Tethys Ocean (Hallam, 1983; Riccardi, 1991; Hillebrandt et al., 1993; Gasparini et al., 2015; Parent et al., 2015).

2.2. The Tithonian to early Valanginian mixed siliciclastic-carbonate system

In the Neuquén Basin, a major flooding episode in the early Tithonian (~148 Ma) was followed by a regression with gently inclined and dominantly NW trending prograding clinoforms continuously filling the basin up to the early Valanginian (~137 Ma) (Fig. 1A-B). This transgressive and regressive system is the result of a second-order eustatic cycle (Legarreta and Uliana, 1991, 1996) with local tectonic influence (Vergani et al., 1995). The system comprises two main stratigraphic units that correspond to different positions within the prograding clinoforms (Fig. 1C). The topset deposits are shallow-water carbonates and siliciclastics of the Picún Leufú and Quintuco Formations, while foreset and bottomset deposits are the organic-rich black shales of the Vaca Muerta Formation (Leanza, 1973; Mitchum and Uliana, 1985; Legarreta and Uliana, 1991; Massaferro et al., 2014; Zeller et al., 2015; Paz et al.,

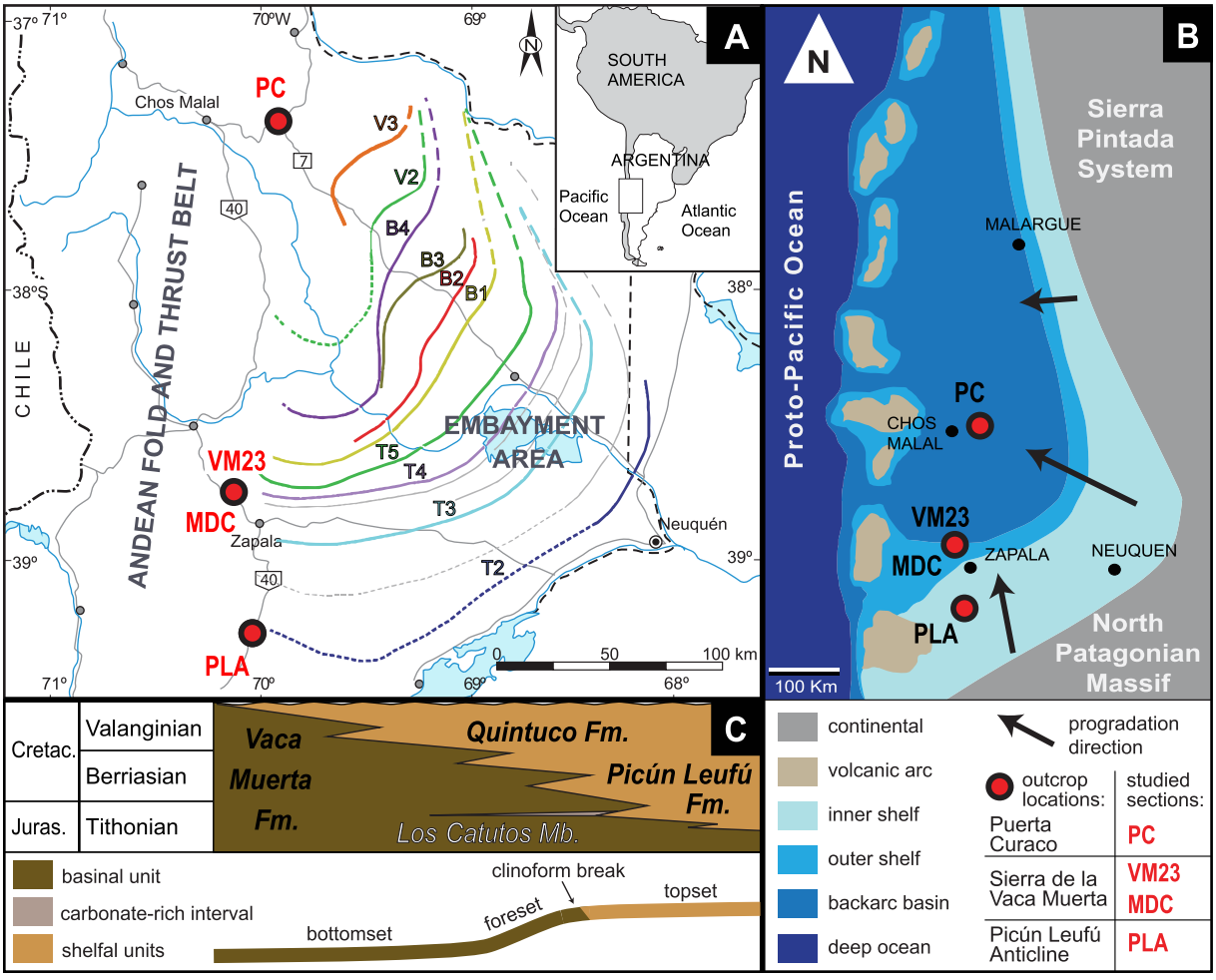

Fig. 1. A) Location map of the Neuquén Basin with the 3 outcrop locations (red dots) and the names of the 4 studied sections. Lines T2 to V3 (T: Tithonian, B: Berriasian, V: Valanginian) are seismic clinoform breaks (modified from Domínguez et al., 2017) showing progradation of the mixed siliciclastic-carbonate system in the subsurface. B) Paleo-geographic reconstruction of the Neuquén Basin for the Tithonian to early Berriasian (modified from Zeller, 2013). C) Lithostratigraphic units and their approximate positions along a clinoform (shelfal units: topset; basinal unit, including carbonate-rich interval: foreset and bottomset). Juras.: Jurassic; Cretac.: Cretaceous. (For interpretation of the references to colour in this figure legend, the reader is referred to the web version of this article.)

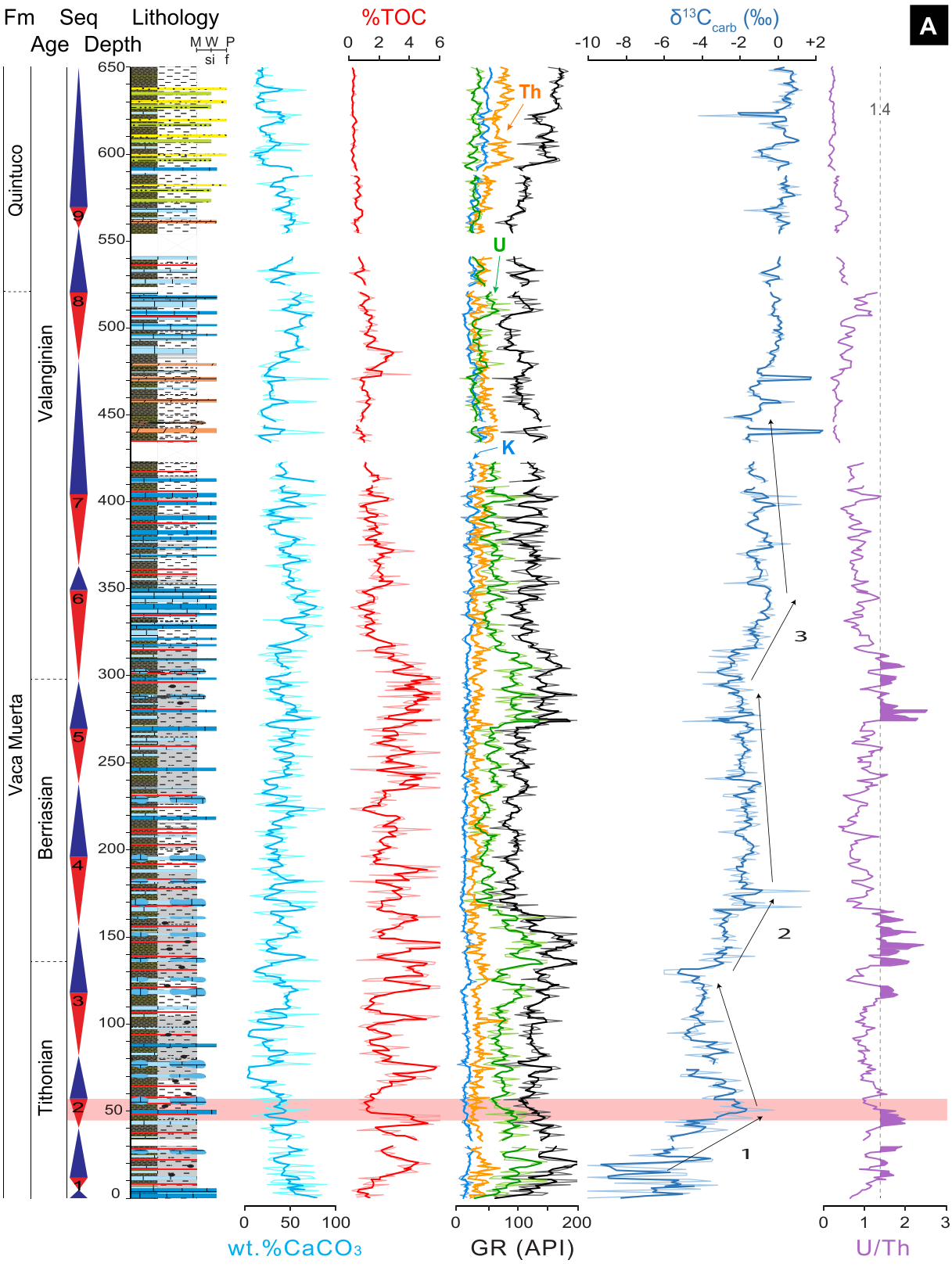

Fig. 2. Stratigraphic sections. A) PC section, and B) MDC section. Profiles of geochemical proxies are carbonate content (wt%$CaCO_3$), total organic content (%TOC), gamma ray (GR) total (black) and spectral (potassium [K, light blue], thorium [Th, orange], uranium [U, green]), $\delta^{13}C$ carbonate isotope values ($\delta^{13}C_{carb}$), and U/Th ratio (U/Th). Profiles include both measured data (except for the U/Th ratio) and calculated 3-point average. Highest U/Th values (> 1.4) are highlighted to indicate the intervals most likely representing truly anoxic conditions. Highlighted in red is the mid-late Tithonian interval considered for proximal-distal analysis in Fig. 4. Fm: Formation, Seq: Sequence. Abbreviations for grain size are M (mudstone), W (wackestone), P (packstone), si (silt), f (fine sandstone). Sections are modified from Rodriguez Blanco (2016) and Rodriguez Blanco et al. (2020), which provide further detail on the sedimentology and sequence stratigraphy. (For interpretation of the references to colour in this figure legend, the reader is referred to the web version of this article.)

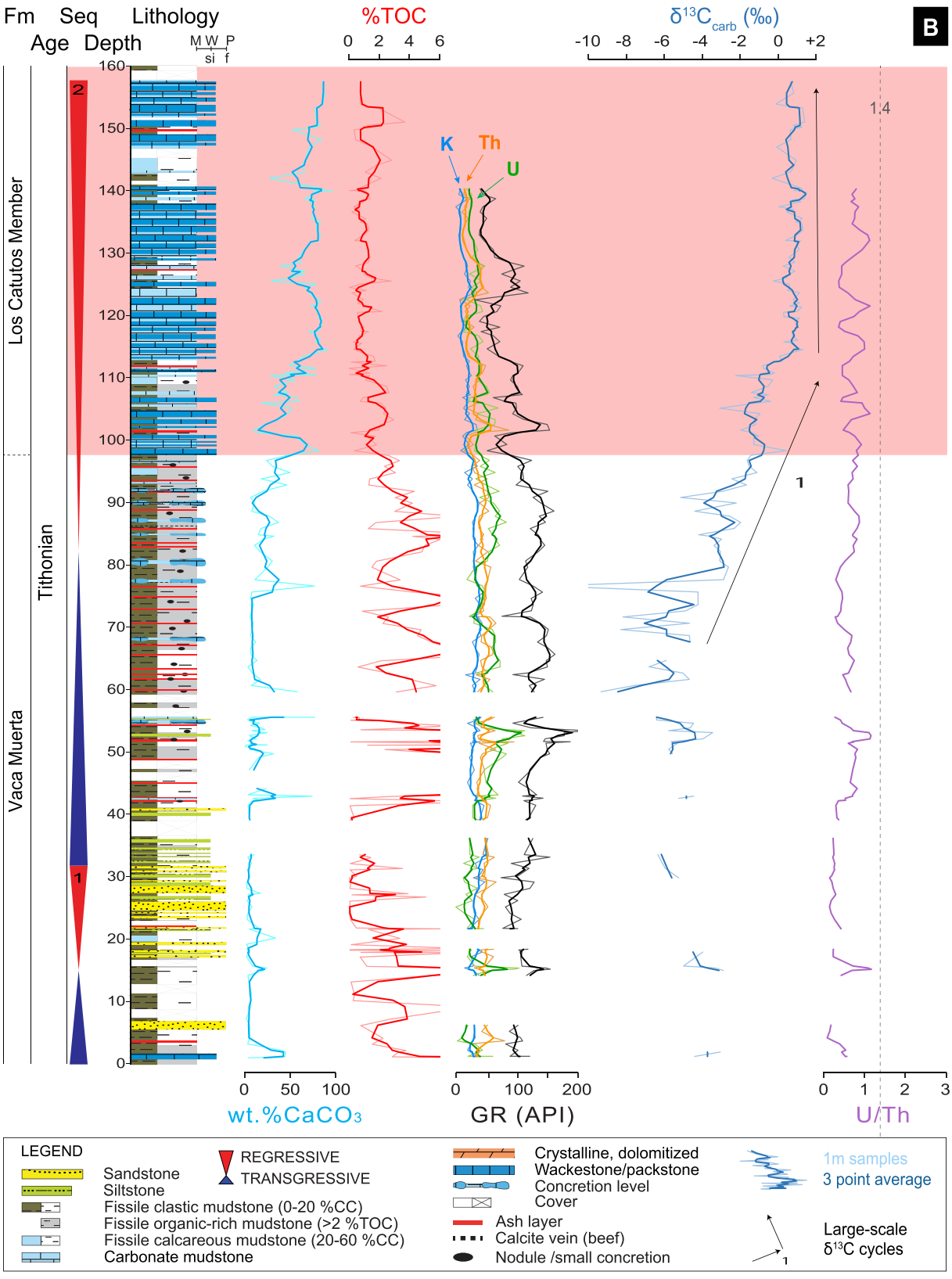

Fig. 2. (*continued*).

2019; Domínguez et al., 2020). Relief estimates between top and base of clinoforms indicate 200 to 400 m of water depth (Mitchum and Uliana, 1985; Minisini et al., 2020). Within the Vaca Muerta Formation, a prominent fine-grained carbonate-rich interval is named the Los Catutos Member (Leanza and Zeiss, 1990), but similar, although younger, intervals occasionally accumulate on the slopes adjacent to carbonate-dominated shelves (Rodriguez Blanco et al., 2020).

2.3. Depositional environment and lithology of the Vaca Muerta Formation

The black shales of the Vaca Muerta Formation accumulated in an epeiric sea connected to the proto-Pacific Ocean through gaps in the magmatic arc (Legarreta and Uliana, 1996; Spalletti et al., 2000; Fig. 1B). Volcanism in the western arc (calc-alkaline series; Rutman et al., 2021) was prevalent throughout the Tithonian and Berriasian (Meissinger and Lo Forte, 2014), evidenced as frequent ash layers alternated with the organic-rich shales. Lithological and geochemical heterogeneity both in depositional cycles and along bottomsets/foresets of the clinoforms suggest variations in depositional paleo-environments driven by changes in sea level, marine currents, climate, sediment flux, etc. (Kietzmann et al., 2011; Zeller, 2013; Spalletti et al., 2000, 2019; Minisini et al., 2020; Otharán et al., 2020; Capelli et al., 2021b).

In central positions of the basin, the deposits of the Vaca Muerta Formation are organic-rich clastic and calcareous mudstones largely devoid of bioturbation, with abundant calcite veins, thin ash layers and calcite concretions (Doyle et al., 2005; Kietzmann et al., 2014; Spalletti et al., 2014; Paz et al., 2019; Minisini et al., 2020; Otharán, 2020; Reijenstein et al., 2020; Capelli et al., 2021a). Redox sensitive elements and organic productivity indicators within the basinal successions point to accumulation in anoxic conditions and low sedimentation rates (Spalletti et al., 2014, 2019; Hernandez Bilbao, 2016; Krim et al., 2019; Capelli et al., 2021b). On the slope, mudstones have lower organic content, are more carbonate-rich but devoid of concretions, and have both trace and body fossils of mollusks indicating dysoxic to oxic conditions (Doyle et al., 2005; Kietzmann et al., 2014; Spalletti et al., 2019; Minisini et al., 2020; Reijenstein et al., 2020).

The lithological variability of the Vaca Muerta Formation is also observable in vertical profiles, which display a strong rhythmic sedimentation pattern (Scasso et al., 2005; Kietzmann et al., 2011; Leanza et al., 2020). Cycles at different scales display partitioning in facies and geochemical proxies between transgressive and regressive portions (Zeller et al., 2015; Rodriguez Blanco, 2016). Transgressive hemicycles are laminated clastic or calcareous TOC-rich mudstones with small concretions, intercalated calcite veins and ash layers. Facies coarsen (silty mudstone) and thicken and/or carbonate content increases (mudstone-wackestone) in the regressive hemicycles. In the basin center, cycle tops are laminated calcareous mudstones with large concretions (Rodriguez Blanco et al., 2022), whereas in more proximal settings they are massive silty layers or wackestone-packstone beds.

3. Materials and methods

A 650 m succession in Puerta Curaco (PC section; Fig. 1A) and a 160 m succession in the southern part of the Sierra de la Vaca Muerta (MDC section; Fig. 1A) were sampled for carbon isotope analysis at 1 m intervals. The PC section in the center of the basin is the more expansive, covering strata from the early Tithonian to the early Valanginian (Fig. 2A). The MDC section, in a relatively more proximal setting, only covers Tithonian strata (Fig. 2B). Shorter sections (~20 m thick) in the Picún Leufú Anticline (PLA section; Fig. 1A) and the northern part of the Sierra de la Vaca Muerta (VM23 section; Fig. 1A) were sampled to investigate lateral isotope variations for a specific interval of mid-late Tithonian age.

In the case of the PLA section in the shelf, the $\delta^{13}C_{carb}$ values were measured only in the fine-grained lithologies (carbonate mudstones and wackestones) to minimize risk of meteoric alteration due to exposure. In the other sections from slope and basin settings, where mudstone and silty-mudstone compositions dominate, samples cover all lithologies with >10 wt% $CaCO_3$, which was the limit to obtain meaningful $\delta^{13}C_{carb}$ values. However, ash layers, calcite veins and concretions were sampled separately and are not part of this analysis. Table 1 shows the provenance of the 814 studied samples, of which 179 correspond to the mid-late Tithonian interval investigated for proximal-distal variations.

Table 1
Number of samples measured in each studied section: Puerta Curaco (PC), Sierra de la Vaca Muerta (SaVM-VM23 and SaVM-MDC) and Picún Leufú Anticline (PLA). For the proximal-distal analysis in Fig. 3, only time-equivalent intervals to the Los Catutos Member were considered (mid-late Tithonian: m-l Tith).

Section	Total samples	Samples for proximal-distal analysis (m-l Tith interval)
PC	591	14 (mid-late Tithonian: 45–57 m)
SaVM - VM23	21	21 (Los Catutos Member: ~72–90 m)
SaVM - MDC	149	91 (Los Catutos Member: ~97–163 m)
PLA	53	53 (mid-late Tithonian: ~448–475 m)

Outcrop samples were pulverized, and carbonate isotopes were measured via dissolution of whole-rock powder in phosphoric acid (Swart et al., 1991) and the CO_2 produced in this process was analyzed on a Finnigan MAT 251. Each run included 25 samples, with 3 standards at the beginning and 2 standards at the end. Data were corrected for any fractionation in the reference gas during the run and reported relative to the Vienna Pee Dee Belemnite (VPDB) scale. Errors on these measurements are <0.1‰ based on replicate analysis.

Samples of all sections had been previously analyzed for carbonate content (wt%$CaCO_3$) and total organic content (TOC). In addition, sections PC and MDC had spectral Gamma Ray (GR) measurements at 1 m intervals, coinciding with each of the sites sampled for geochemical analyses. Sections had been previously studied for sedimentary facies and placed within a sequence-stratigraphic framework [further detail is in Zeller, 2013 for PLA, and Rodriguez Blanco, 2016 and Rodriguez Blanco et al., 2020 for PLA, MDC, VM23 and PC]. Ages were constrained by nearby biostratigraphic sections from the literature (Aguirre Urreta and Vennari, 2013; Aguirre Urreta et al., 2014).

PC and MDC that are the most complete sections in terms of thickness and measured proxies, are described in more detail (see Results 4.1) and investigated for vertical trends in $\delta^{13}C_{carb}$ values (see Results 4.2). Specific intervals of mid-late Tithonian age (highlighted in red in Fig. 2A-B) were also analyzed for proximal-distal variations in $\delta^{13}C_{carb}$ values (see Results 4.3). The other two shorter sections, PLA and VM23, are only briefly described (see Results 4.1) and investigated for lateral variations in $\delta^{13}C_{carb}$ values along the proximal-distal transect of mid-late Tithonian age (see Results 4.3).

4. Results

4.1. The sedimentary succession in the studied outcrop locations

Given the strong cyclic character of the analyzed successions (see Section 2.3), this part of the work describes each logged section in terms of basic transgressive-regressive cycles. These high-frequency cycles display facies partitioning and differences in wt%$CaCO_3$ and TOC between transgressive and regressive hemicycles. Facies and geochemical trends (wt%$CaCO_3$ and TOC) in cycle sets and sequences replicate those of the high-frequency cycles.

4.1.1. Puerta Curaco (PC section)

The sedimentary succession in the Puerta Curaco area (Fig. 2A) covers the entire Vaca Muerta Formation and the lower part of the Quintuco Formation, in a shallowing upward trend that is the result of the progradation of the system from the early Tithonian to the early Valanginian. In the basal 300 m of the PC section, the lithology is an alternation between fissile mudstones with high organic content (avg. 2–6% TOC), either clastic (wt%$CaCO_3$ < 15%) or calcareous (wt% $CaCO_3$ 15–50) in composition, and silty-mudstones or mudstone-wackestones towards cycle tops. The basal fissile mudstones dominate most of the stratigraphic cycles. Pyrite is abundant in the fissile mudstones, and lamination results from variations in content of detrital material, organic matter, and/or coccolithic aggregates. Bioclasts are

mostly pelagic (e.g., ammonites, radiolarians, fish scales). These organic-rich facies are associated with stratigraphically aligned concretions of variable sizes (few cm to >1 m), calcite veins, and thin ash layers, which can be either calcite cemented or replaced with clays. This part of the section represents the more distal setting and consists of sequences 1 to 5.

From 300 to 520 m, the succession is a cyclic alternation between fissile organic-rich mudstone in transgressive portions and highly continuous ~0.3 m thick skeletal or peloidal wackestone/packstone beds (wt%$CaCO_3$ > 60) in regressive portions. The carbonate beds are massive or slightly laminated, commonly bioturbated, with silt-size quartz and carbonate grains, and have 1–2% TOC and occasional pyrite. Common bioclasts include ammonites, radiolarians, micro-crinoids, bivalves and sponge spicules. An exception occurs in the 420-480 m interval, where some carbonate beds are completely replaced by crystalline dolomite. The carbonate-rich intervals occur in the regressive part of sequences 6 to 8 and are interpreted as distal periplatform deposits shed from the carbonate-dominated shelves located along the eastern side of the basin. Above 520 m the system becomes increasingly siliciclastic, alternating greenish mudstones, siltstones and cross-stratified fine sandstones of the Quintuco Formation deposited on a shallow shelf.

4.1.2. Sierra de la Vaca Muerta (MDC and VM23 sections)

In the southern part of the Sierra de la Vaca Muerta (MDC section) the sedimentary succession starts with a clastic-dominated, relatively coarse-grained interval that consists of organic-rich mudstones grading to siltstones and massive sandstones (Fig. 2B). These sediments were shed from a clastic-dominated mixed-shelf in the south of the basin.

Between 40 and 95 m, the basinal facies consist of organic-rich (TOC > 2% and locally up to 10%) fissile mudstones with abundant concretions, and ash layer commonly replaced with clays. These facies are very similar to those described for the lower part of the PC section (0-300 m), and also represent the more distal environment.

Above 95 m (Fig. 2B), the succession transitions into the limestones of the Los Catutos Member of mid-late Tithonian age. Stratigraphic cycles in this interval have a very thin (or absent) transgressive portion that is a fissile and organic-rich calcareous mudstone, and a regressive portion that consists of highly continuous and thick (up to 1.2 m), massive or slightly laminated carbonate beds. These skeletal or peloidal wackestone/packstone beds (mean 85 wt%$CaCO_3$) are commonly bioturbated and with ~1% TOC. Skeletal fragments are abundant and include ammonites, radiolarians, micro-crinoids, bivalves and sponge spicules. Silt-size quartz is common, and pyrite is locally abundant. The presence of large-scale sedimentary features as slump scars, slides, and small channels down cutting into the Los Catutos Member point to a slope position near the shelf break.

In the northern part of the Sierra de la Vaca Muerta (VM23 section), the mid-late Tithonian Los Catutos Member is reduced in thickness to approximately 20 m and consists of a cyclic alternation of relatively thick (up to 1.5 m) organic-rich fissile mudstones in transgressive portions and ~ 0.3 m thick slightly laminated skeletal or peloidal wackestone beds (mean 65 wt%$CaCO_3$) towards cycle tops. These carbonate beds are rarely bioturbated, have TOC values between 1 and 3% and their skeletal content, although similar to the MDC section, is not as abundant. The sedimentary succession in VM23 is very similar to the carbonate-rich intervals that occur in the PC section between 300 and 520 m, and is also interpreted as a distal periplatform deposit.

4.1.3. Picún Leufú Anticline (PLA section)

The studied mid-late Tithonian interval in the Picún Leufú Anticline is a ~ 20 m thick pure carbonate package that forms part of the Picún Leufú Formation. The sedimentary facies are mudstone-wackestones in transgressive hemicycles and bivalve-oyster floatstones and cross-bedded oolitic grainstones towards cycle tops (mean 86 wt%$CaCO_3$). This interval represents the most proximal setting among the studied sections and corresponds to a tidally dominated shelf environment.

4.2. Cycle partitioning and vertical trends in $\delta^{13}C_{carb}$ values

The high-frequency cycles described in Section 4.1, which exhibit partitioning in facies, carbonate content and TOC between transgressive and regressive portions, also show partitioning in $\delta^{13}C_{carb}$ values. Fig. 3 displays cross plots of carbonate content vs. TOC and $\delta^{13}C_{carb}$, and $\delta^{13}C_{carb}$ vs. TOC for a reduced dataset of mid-late Tithonian age in each of the studied locations. Samples from transgressive hemicycles are in blue, and samples from regressive hemicycles are in yellow (for most of the regressive) and red (for cycle tops). Transgressive portions of cycles tend to have higher TOC and lower $\delta^{13}C_{carb}$ values while regressive portions, and especially cycle tops, have both higher wt% $CaCO_3$ and $\delta^{13}C_{carb}$ values (Fig. 3). As with the sedimentary facies, cycle sets and sequences also display higher $\delta^{13}C_{carb}$ values towards tops, while the more negative $\delta^{13}C_{carb}$ values tend to be associated with transgressive portions (Fig. 2).

In a larger scale, the profile of $\delta^{13}C_{carb}$ values in Puerta Curaco (Fig. 2A) shows an overall increasing trend from the early Tithonian to the early Valanginian. The first 420 m of PC section (sequences 1 to 7) exhibit negative $\delta^{13}C_{carb}$ values between −8 and − 1‰ on average, which are arranged in 3 large-scale increasing-decreasing cycles. Variations in $\delta^{13}C_{carb}$ values are larger in the increasing parts of the aforementioned cycles (from base to top 4.8, 2.9 and 2‰), and smaller in the corresponding decreasing portions (2.2, 1 and 0.7‰). Minimum $\delta^{13}C_{carb}$ values occur at the inflection points between cycles. The oldest minimum is in the early to middle Tithonian (sequence 1 and early transgressive portion of sequence 2), the second is near the Tithonian-Berriasian boundary (transgressive portion of sequence 4), and the third is near the Berriasian-Valanginian boundary (maximum flooding and early regressive portion of sequence 6). Around 450 m, a change in $\delta^{13}C_{carb}$ values between −2 and 0‰ takes place, although partially masked by poor exposure and with locally occurring very high $\delta^{13}C_{carb}$ values (+4 to +6‰) in dolomitized beds. Above 490 m, the $\delta^{13}C_{carb}$ values are fairly constant between 0 and +1‰.

The high-resolution profile of $\delta^{13}C_{carb}$ values in the MDC section (Fig. 2B) only covers strata from Tithonian age (Sequences 1 and 2). The lower part of the MDC section (0-40 m) has very few $\delta^{13}C_{carb}$ measurements due to the very low carbonate content of that part of the succession (wt% $CaCO_3$ < 10). Between 40 and 80 m approximately, the profile exhibits very negative $\delta^{13}C_{carb}$ values (−5.8‰ on average) followed by a significant increasing change up to an average value of +0.8‰. This inflection point in the $\delta^{13}C_{carb}$ profile corresponds to the transgressive portion of sequence 2. Upwards in the section, the $\delta^{13}C_{carb}$ values in the Los Catutos Member remain constant around +0.8‰.

4.3. Lateral changes in $\delta^{13}C_{carb}$ values along the mid-late Tithonian interval

This section seeks to analyze the measured $\delta^{13}C_{carb}$ values in different parts of the basin for a selected time interval of mid-late Tithonian age (Fig. 4). With that purpose, we will focus on the average values of two intervals already described when analyzing vertical trends in PC and MDC sections (red-colored in Fig. 2A-B), and in the interval values of the shorter sections VM23 and PLA. The studied transect, from south to north, thus covers shelf, slope and basin settings (Figs.1B and 4).

The distribution of the measured $\delta^{13}C_{carb}$ values for the mid-late Tithonian interval in the four studied sections appears in Fig. 5. In the shelf (PLA section), >90% of the measured $\delta^{13}C_{carb}$ values ($n = 53$) are between +1 and + 3‰. In the proximal periplatform setting (MDC section), the time-equivalent interval ($n = 91$) shows $\delta^{13}C_{carb}$ values between −3 and + 2‰. Approximately 70% of those measurements have positive values between 0 and + 2‰, while the remaining 30% varies mostly between −2 and 0‰. In the distal periplatform setting

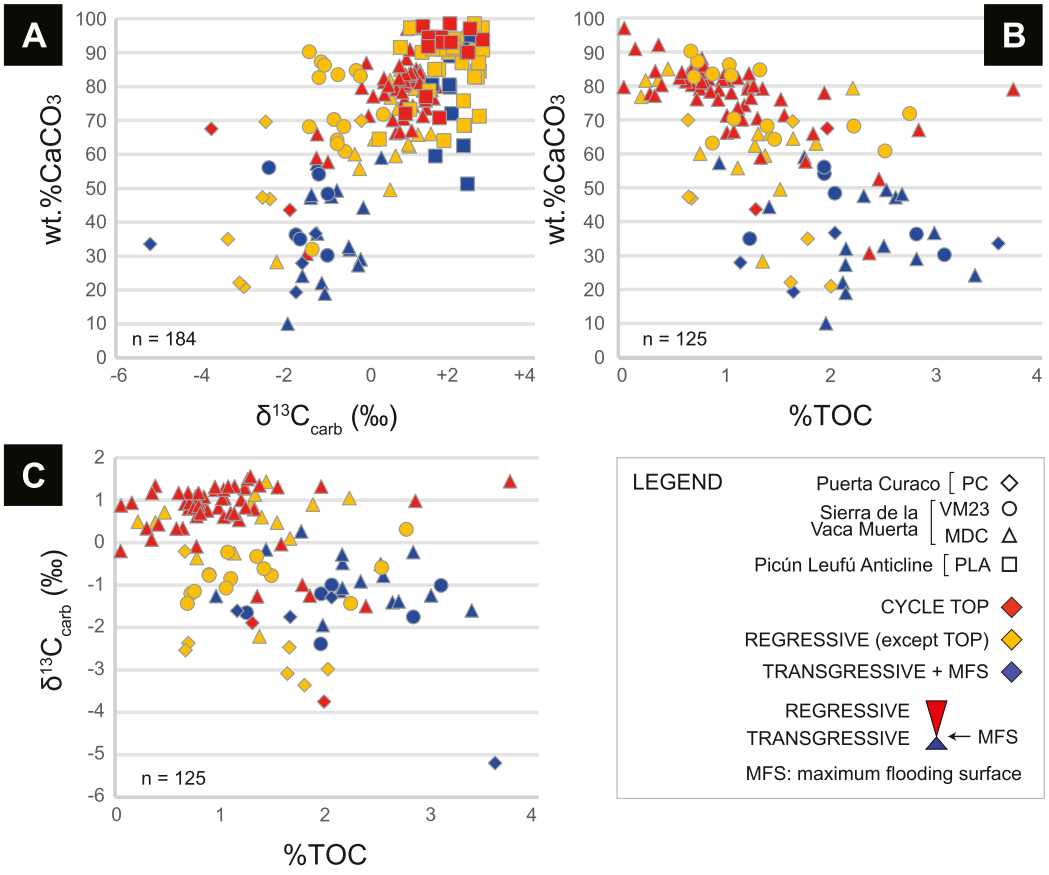

Fig. 3. Cross-plots of A) $\delta^{13}C_{carb}$ vs. wt%$CaCO_3$, B) TOC vs. wt%$CaCO_3$, and C) TOC vs. $\delta^{13}C_{carb}$ for the analyzed mid-late Tithonian interval (Fig. 4). Colour-coding refers to the position of the sample within the sequence-stratigraphic cycles. Part of the isotope data and wt%$CaCO_3$ of PLA come from Afsar (2010). Notice that PLA lacks TOC measurements.

(VM23 section), 90% of the measured $\delta^{13}C_{carb}$ values ($n = 21$) vary between −2 and 0%. In the center of the basin (PC section), the time-equivalent interval ($n = 14$) exhibits 85% of the $\delta^{13}C_{carb}$ values in the −4 to −1‰ range. This basinward decrease in $\delta^{13}C_{carb}$ values is coupled with a decrease in wt%$CaCO_3$ and a relative increase in TOC (Fig. 3).

5. Discussion

5.1. Comparison with Tethyan $\delta^{13}C_{carb}$ values

The Neuquén basin in Argentina contains a continuous marine succession of mudstones with a $\delta^{13}C_{carb}$ record of the Late Jurassic to the Early Cretaceous. The $\delta^{13}C_{carb}$ values from this Southern Ocean basin potentially provide insight into global carbon cycle dynamics when compared to the values from the equatorial realm. In epicontinental settings, however, local controls on $\delta^{13}C_{carb}$ values must be considered. It is often assumed that a) the magnitude of variation in $\delta^{13}C_{carb}$ values is amplified in epicontinental settings compared to pelagic settings, especially when that magnitude is globally low as in the Tithonian to Valanginian time interval, and b) that is "exceptionally difficult to attribute the entirety of the $\delta^{13}C_{carb}$ excursion to diagenetic or local carbon cycling effects" (Cramer and Jarvis, 2020; and references therein). The $\delta^{13}C_{carb}$ profile of the PC section in the Neuquén Basin, however, is radically different from the Tethyan profile (Fig. 6).

For the Tithonian to Valanginian interval, the Tethyan profile shows a slightly decreasing trend with values between ~ + 2.5 and + 1‰ (Fig. 6). Minor events in the middle and late Berriasian (MBeE and LBeE, respectively), and a major increase up to +3 and + 4‰ in the upper Valaginian (Weissert event) would be the result of global perturbations in the carbon cycle (Lini et al., 1992; Föllmi et al., 1994; Erba et al., 2004; Bodin et al., 2009; Cramer and Jarvis, 2020). In contrast, the profile from the PC section in the Neuquén Basin displays much more negative $\delta^{13}C_{carb}$ values with 3 large-scale increasing-decreasing cycles (0-420 m), and an overall increasing trend (Fig. 6). The most negative $\delta^{13}C_{carb}$ values will be discussed in Section 5.2. The increasing trend above the 3rd large-scale cycle might be due to the more humid conditions proposed for the Valanginian (Föllmi, 2012).

Although $\delta^{13}C_{carb}$ values in the PC section are more negative than in the Tethyan profile, thus suggesting a strong diagenetic overprint of the Neuquén strata, we cannot rule out that some of the variations in the PC section might reflect processes that are global in nature. For example, the position of more positive $\delta^{13}C_{carb}$ values in the middle Berriasian is fairly close to the Middle Berriasian event, and the slight negative shift of $\delta^{13}C_{carb}$ values at the top of the Berriasian coincide with the Late Berriasian event in the Tethys, although the values are still much more negative (Fig. 6). The chronology of the PC profile is, however, approximate based on chronostratigraphic interpretations from other authors (see explanation in caption of Fig. 6), which produces some uncertainty for correlating the PC section to those outside of the Neuquén basin. But even if the curve would shift a bit in age, the local imprint on the $\delta^{13}C_{carb}$ values of the PC section is so dominant that the global signal of carbon cycling in this time interval cannot be extracted.

A most interesting aspect of the Tithonian and early Berriasian time is that deposition of organic-rich mudstones occurred in several semi-restricted basins of the world (seaways and epicontinental seas; see Föllmi, 2012 and references therein). Like the Neuquén basin, these basins were susceptible to become density-stratified and develop dys-to anaerobic conditions in deeper waters. High burial rates of organic

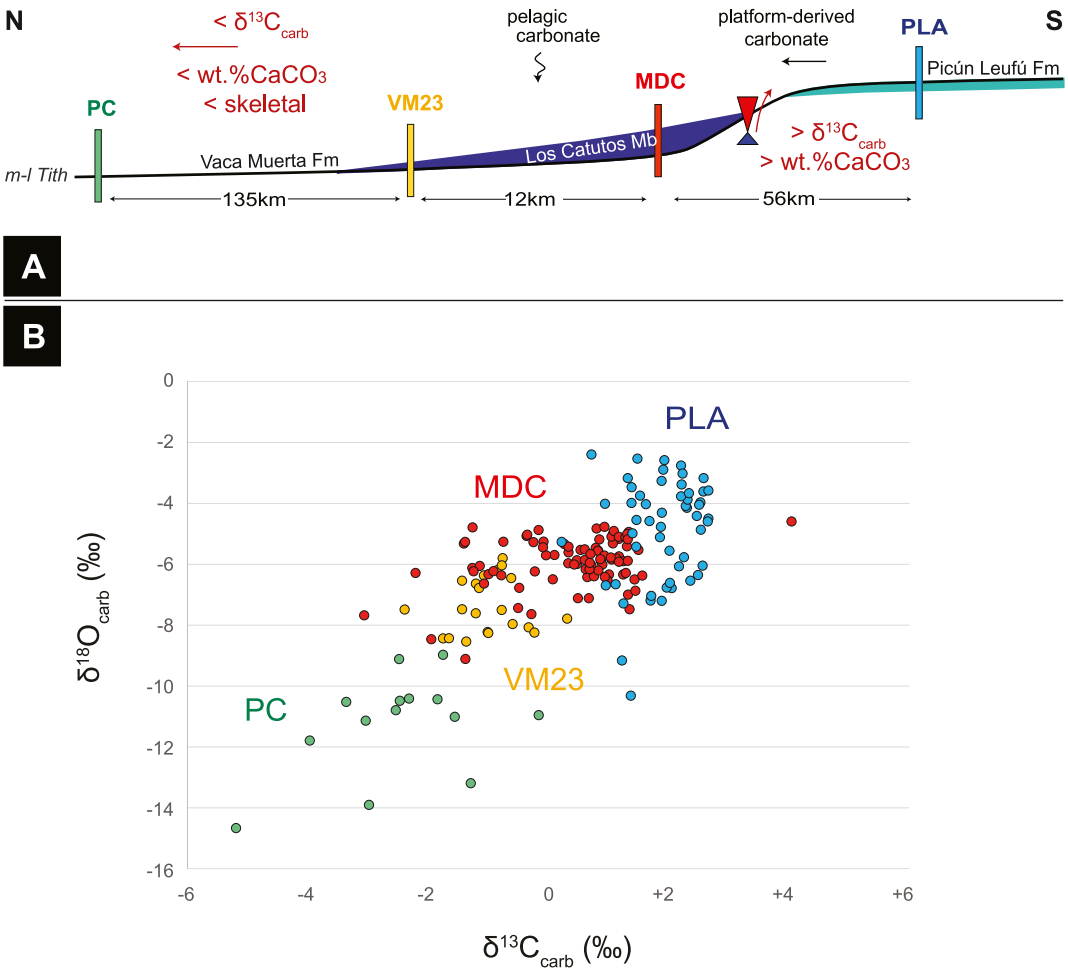

Fig. 4. A) Schematic north-south outcrop cross-section (see Fig. 1 for location) for the analyzed mid-late Tithonian interval (m-l Tith). Proximal-distal and cyclic behavior of carbonate content (wt%$CaCO_3$), skeletal content and $\delta^{13}C_{carb}$ values are also schematized. Blue and red triangles represent transgressive and regressive portions respectively. B) Cross-plot of $\delta^{13}C_{carb}$ vs. $\delta^{18}O_{carb}$ for the mid-late Tithonian interval. Samples are colored according with the outcrop location to highlight proximal-distal variations. (For interpretation of the references to colour in this figure legend, the reader is referred to the web version of this article.)

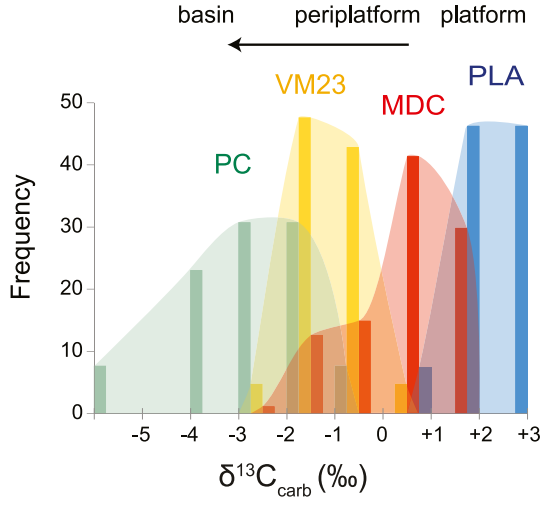

Fig. 5. Distribution of the $\delta^{13}C_{carb}$ values for the investigated mid-late Tithonian interval in each of the outcrop sections. Columns in each histogram bin (e.g., −2 to −1‰) correspond, from left to right, respectively to PC, VM23, MDC and PLA (the latter without data in the specified bin). Part of the isotope data of PLA come from Afsar (2010).

carbon in the world oceans typically produce positive excursions in the rock record, which have been explained by a relative increase in the $^{13}C/^{12}C$ ratio of marine waters, as ^{12}C was preferentially removed via organic matter burial (Scholle and Arthur, 1980; Jenkyns and Clayton, 1997). Even though several major source-rocks are Tithonian-early Berriasian in age, the Tethyan $\delta^{13}C_{carb}$ record (Fig. 6) does not reflect this phase of removal of organic carbon from the global ocean. Föllmi (2012) interpreted this lack of record to be the result of a generally arid climate coupled with low biogeochemical weathering rates and nutrient fluxes. These conditions would have precluded major organic carbon production and preservation in the world oceans during the Tithonian and early Berriasian, unless associated with local preservation factors such as in well-stratified seas. Föllmi (2012) also speculates that even if the local deposition of organic matter would have been sufficiently important as to increase the $\delta^{13}C_{carb}$ values, compensatory effects such as increased marine carbonate deposition or reduced organic burial in continental sediments would have played a role in buffering the global record.

5.2. *The basinal negative $\delta^{13}C_{carb}$ values*

A significant difference in $\delta^{13}C_{carb}$ values exists between the basinal organic-rich mudstones and the shelf carbonates (Fig. 5). Since the surface water of the Neuquén Basin was open marine and connected to the Proto Pacific Ocean (Legarreta and Uliana, 1996; Gasparini et al.,

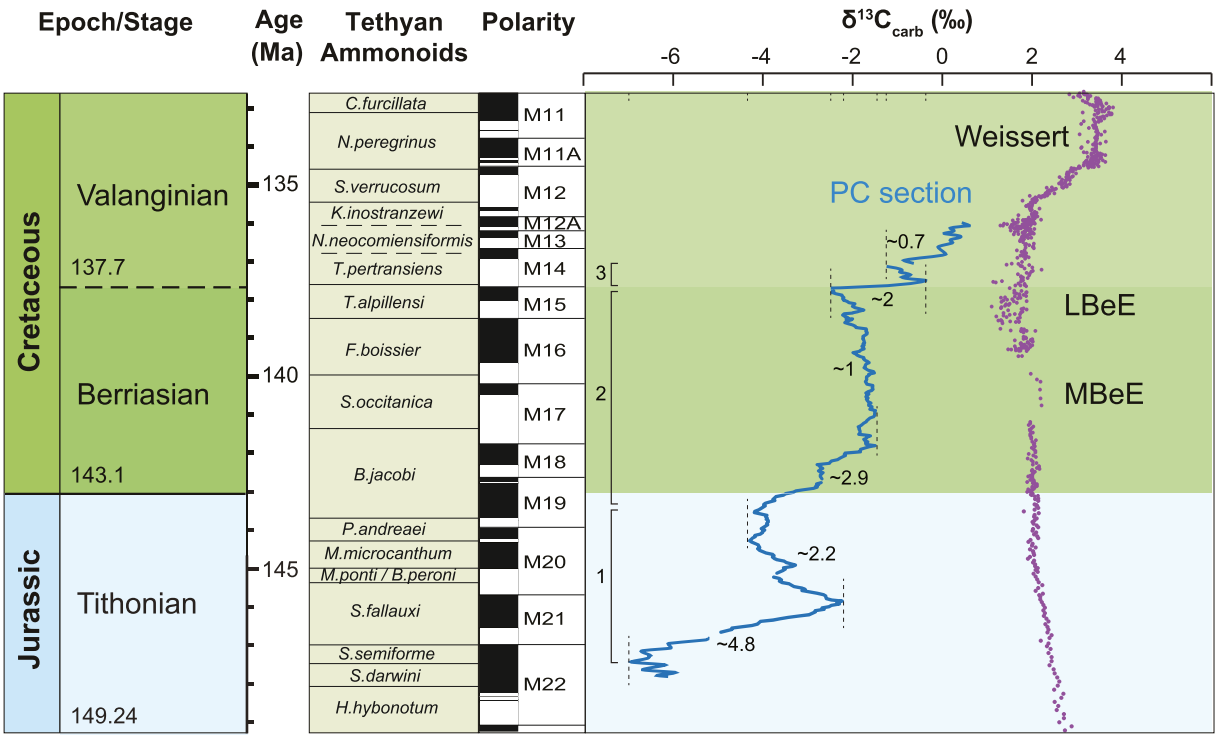

Fig. 6. Comparison of the $\delta^{13}C_{carb}$ values of the Tethys (in purple; Cramer and Jarvis, 2020) and those of PC section in the Neuquén basin (in blue; this work). The PC profile displayed here is a 15-point average of the measured values, to emphasize main trends. Figure is modified from the Geological Time Scale (GTS) 2020. Polarity and ammonite data are from Hesselbo et al. (2020) for the Jurassic and Gale et al. (2020) for the Cretaceous. Positioning of PC is approximate: base of the section was considered within the *S.darwini* ammonite zone (Aguirre Urreta et al., 2014), in the middle portion of polarity chron M22 (Hesselbo et al., 2020). Tithonian, Berriasian and Valanginian segments were stretched/shortened to match their respective boundaries (assumption of constant depositional rate). The top of the curve is placed approximately within the former B.campilotoxus ammonite zone (Aguirre Urreta et al., 2008), now *N.neocomiensiformis* and *K.inostranzewi* zones (Reboulet et al., 2014) corresponding respectively to polarity chrons M13- M12A and M12A- M12 (Gale et al., 2020) earlier than the Weissert Event. Large-scale cycles from Fig. 2 are indicated with brackets, and dotted vertical lines represent extreme average $\delta^{13}C_{carb}$ values for the increasing/decreasing portion of each cycle. Average ranges are provided for each segment. (For interpretation of the references to colour in this figure legend, the reader is referred to the web version of this article.)

1997), it is possible that the $\delta^{13}C_{carb}$ values measured in the PLA section are reflective of global ocean $\delta^{13}C_{DIC}$ values and are consistent with the Tethyan $\delta^{13}C_{carb}$ values (Weissert and Erba, 2004; Katz et al., 2005; Grabowski et al., 2019). On the other hand, those found in the basinal sites (VM23 and PC sections) are considerably more negative reflecting processes occurring in the deeper waters of the Neuquén basin.

Several processes can account for the negative $\delta^{13}C_{carb}$ values of bulk samples found in the Vaca Muerta Formation (Wendler, 2013; Ahm and Husson, 2022), including (i) alteration by meteoric fluids, (ii) variations in the origin of carbonate material, and (iii) diagenetic alteration and authigenic precipitation.

i. Exposure to meteoric waters

The typical influence of meteoric diagenesis on both the $\delta^{13}C_{carb}$ and $\delta^{18}O_{carb}$ values of a carbonate sequence is for the values to become more negative, according to models proposed by Allan and Matthews (1982) and Lohmann (1988). In these models, the meteoric fluids have more negative $\delta^{18}O_{carb}$ and $\delta^{13}C_{carb}$ values, with such signals being derived from the local rainfall and the oxidation of local organic materials. In the case of the data we investigated, the site most likely to have been influenced by meteoric fluids is PLA, which is located on the southern shelf and therefore potentially affected by glacio-eustatic sea level changes. In contrast, sites MDC and VM23 are situated on the slope with site PC located in the basin and were never exposed (Minisini et al., 2020). While the $\delta^{18}O_{carb}$ values in PLA (−2 to −8 ‰, Fig. 4) could be interpreted as having been influenced by meteoric fluids, such an interpretation is contrary to the $\delta^{13}C_{carb}$ values being similar to estimates of the $\delta^{13}C_{carb}$ values of carbonates formed in equilibrium with the global ocean during the Late Jurassic (Saltzman and Thomas, 2012; Cramer and Jarvis, 2020). The similarity of the values suggests that the $\delta^{13}C_{carb}$ values have not been altered. As processes involving meteoric fluids would have lowered both the $\delta^{18}O_{carb}$ and $\delta^{13}C_{carb}$ values, it follows that meteoric diagenesis is unlikely to have caused lower $\delta^{13}C_{carb}$ values not only in the PLA section, but also in the other sections which would have been less susceptible to meteoric influence by virtue of their positions relative to the shelf margin. While it is possible that the rocks were altered by meteoric fluids in a significantly later period, there is no petrographic evidence of this and calcite veins have very elevated clumped isotopic temperatures suggesting a hydrothermal origin (Weger et al., 2019). Thus, the low $\delta^{18}O_{carb}$ values in all sections are likely to have resulted from recrystallization during burial in a closed system under the influence of a geothermal gradient. Such processes would have not influenced the original $\delta^{13}C_{carb}$ values.

ii. Compositional changes between platform and pelagic-derived carbonate

The difference in the $\delta^{13}C_{carb}$ values of biogenic carbonate formed on the carbonate platform compared to that of pelagic carbonate might have played a role in explaining some of the difference observed between the shallow proximal site (PLA) and the deeper basinal site (PC). Platform carbonates such as the Great Bahama Bank (Swart and Eberli, 2005; Christ et al., 2012) generally have more positive $\delta^{13}C_{carb}$ values when compared to pelagic material and therefore at least a portion of the lower values in the deeper PC sections might have been influenced by this mechanism.

iii. Anoxic remineralization of organic carbon and consequent precipitation of authigenic carbonate

In the absence of oxygen, sulfate and other electron acceptors can be used to remineralize organic matter, and consequently increase the alkalinity of the pore waters. The bicarbonate produced in such processes will have more negative $\delta^{13}C_{carb}$ values than those in the dissolved inorganic carbon (DIC) of the surface waters (Fig. 7) and therefore affect the $\delta^{13}C_{carb}$ values of any authigenic carbonate formed. In the presence of Fe, the concomitant precipitation of sulfide minerals such as pyrite increases pH, which in turn leads to carbonate supersaturation and precipitation of early diagenetic carbonates with even more negative $\delta^{13}C_{carb}$ values (Sun and Turchyn, 2014). All the key aspects involved in this process (sulfate reduction, organic matter accumulation, pyrite precipitation) occur in the Vaca Muerta Formation. Hence, the negative $\delta^{13}C_{carb}$ values in the Neuquén basin are interpreted to be mostly the result from the precipitation of authigenic carbonate driven by bacterially mediated decomposition of organic matter in sulfate-reducing conditions (Raiswell, 1976). Since most of the organic-rich succession is typically associated with abundant ash layers (Fig. 2), an additional source of isotopically negative carbon might be volcanic gases including CO_2 and CH_4. Anaerobic oxidation of the methane has been implicated in the formation of carbonate cemented ash layers (Rutman et al., 2021). However, with the exception of the interval between 100 and 150 m in the PC section, where there is a local increase in the amount of calcite-cemented ash beds, there is no clear relation between vertical changes in the abundance of ash layers and the changes in $\delta^{13}C_{carb}$ values (Fig. 2),

5.2.1. Extensive sulfate reduction in the basin setting

In the basin setting (0-300 m in PC section, Fig. 2A), abundant concretions (~85 wt%$CaCO_3$) with negative $\delta^{13}C_{carb}$ values (McNeill et al., 2016) occur associated with the laminated organic-rich mudstones (Rodriguez Blanco et al., 2022). The laminated mudstones bend around the concretions indicating that the cementation process took place at shallow depth before significant compaction. The $\delta^{13}C_{carb}$ values of the concretions support the early diagenetic origin of the carbonate, primarily through bacterial oxidation of organic matter and reduction of seawater sulfate (Raiswell, 1976; Coleman and Raiswell, 1981). In addition, the $\delta^{13}C_{carb}$ values measured in the matrix of Tithonian wackestone-packstones in the central part of the basin (Pampa Tril, ~25 km north from PC section; Lanz et al., 2021) vary between −1 and -8‰, suggesting similar early diagenetic reactions to those forming the concretions. These $\delta^{13}C_{carb}$ values coincide with those measured in calcite cemented ash layers (Rutman et al., 2021), and with our measurements from both laminated organic-rich mudstones and wackestone-packstones (Fig. 2).

The laminated organic-rich mudstones in basinal and distal periplatform settings (the first 520 m of the PC section and the 40-97 m interval in MDC section, Fig. 2), are typically devoid of bioturbation, have >2% and locally up to >6% of TOC, and framboidal pyrite is commonly present. These facies also show high values of V, Mo and U/Th, indicative of more reducing conditions (Spalletti et al., 2014, 2019; Krim et al., 2017, 2019; Capelli et al., 2018, 2021b), and high (Ni + Cu)/Al values indicative of greater bioproductivity (Spalletti et al., 2019; Brisson et al., 2020; Capelli et al., 2021b). Furthermore, euxinic conditions have been interpreted during the initial flooding of the basin in the early Tithonian, based on marked enrichments in redox-sensitive and/or sulfide-forming trace metals (Legarreta and Villar, 2015; Krim et al., 2017, 2019; Capelli et al., 2018). This evidence supports a model of highly productive surface waters, high flux of organic matter to the sea bottom, relatively low sediment supply, and the development of anoxic bottom waters during the deposition of the Vaca Muerta Formation (Fig. 7). The accumulation of ash beds in the basin might have contributed to the development of anoxia by hindering oxygen circulation to the underlying sediments (Capelli et al., 2021a; Rutman et al., 2021).

In contrast, in the periplatform setting alternating periods of anoxia-dysoxia might have occurred. In distal periplatform settings (VM23 section, Fig. 4; 300-520 m in PC section, Fig. 2) the laminated organic-rich mudstones alternate with bioturbated wackestone-packstone beds, but in proximal periplatform settings (97–160 m in MDC section, Figs. 2B and 3), the carbonate beds are much thicker and dominate most of the transgressive-regressive cycles. In these near-slope environments, the occurrence of limestones with both trace and body fossils of mollusks, together with higher P concentrations and a relative decrease in

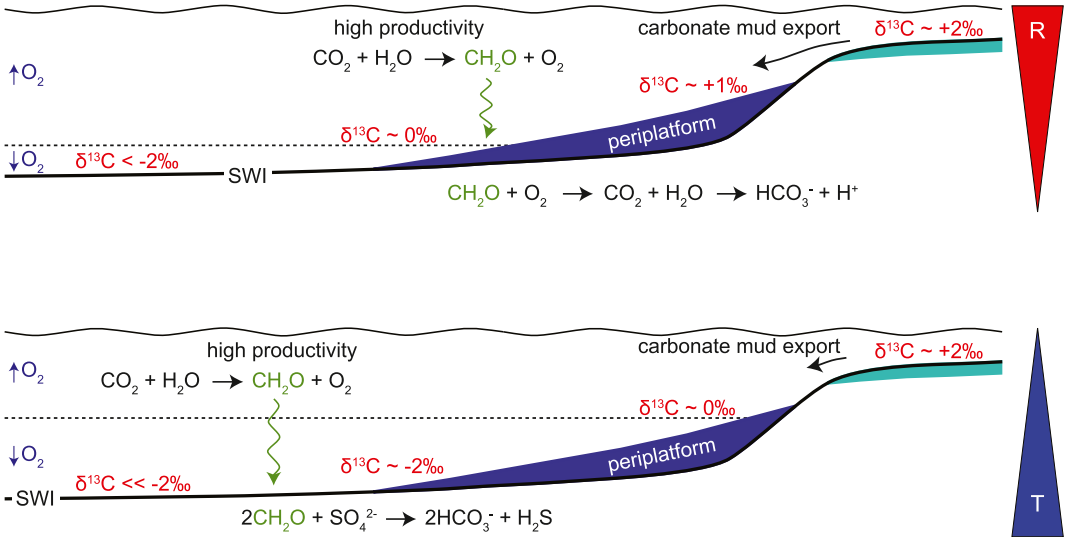

Fig. 7. Proposed model to explain the basinal highly negative values. Organic matter (green) sink through the water column and undergo remineralization, either during sinking or when reaching the sea bottom. Whether the degradation of the organic matter takes place in the presence of oxygen (above) or sulfate (below), the result will be isotopically negative alkalinity. The HCO_3^- thus generated will combine with Ca^{2+} from the seawater to produce isotopically negative carbonates. Indicated $\delta^{13}C_{carb}$ values of the proximal setting (~ +2‰) are characteristic of normal seawater for the Tithonian-early Valanginian, but more negative values are expected basinward as carbonate mud exported from the platform is mixed with carbonate altered by organic matter in anoxic/dysoxic bottoms. SWI: sediment-water interface. The dotted line corresponds to the chemocline, whose position is expected to change in transgressive (below) vs. regressive (above) conditions. (For interpretation of the references to colour in this figure legend, the reader is referred to the web version of this article.)

the abundance of redox proxies (Mo, V, U) indicate that dysoxic (and even mildly oxic) conditions alternated with the anoxic periods (Doyle et al., 2005; Krim et al., 2017; Spalletti et al., 2019; Capelli et al., 2021b). These alternating periods of anoxia-dysoxia point to modifications in the position of the chemocline and/or mixing with oxygenated waters (Fig. 7), which might be driven by changes in relative sea-level, climate, and/or sea-water circulation patterns.

5.3. The origin of stratigraphic changes in $\delta^{13}C_{carb}$ values

The overall increasing trend in the $\delta^{13}C_{carb}$ values of the PC section mirrors the shallowing upward trend of the system, from basinal to periplatform deposits (Fig. 2). A significant environmental change towards more oxygenated conditions, a humid climate and higher sedimentation rates is interpreted for the facies of the Quintuco Formation based on important reductions in TOC and redox proxies, presence of kaolinite, and increments in detrital sedimentation (Capelli et al., 2021b). This climatic change does not have a clear expression in the $\delta^{13}C_{carb}$ record of the PC section, which transitions more or less smoothly towards positive values, from approximately −1.5‰ in the upper part of the Vaca Muerta Formation to ~0.5‰ in the Quintuco Formation (Fig. 2).

Within the overall increasing trend of $\delta^{13}C_{carb}$ values, the 3 large-scale increasing-decreasing $\delta^{13}C_{carb}$ cycles between 0 and ~ 520 m in PC section (Fig. 2) represent variations that took place under generally oxygen-deficient conditions. However, facies and geochemical proxies of this interval (Section 5.2.2) indicate alternated periods of anoxia and dysoxia (Jones and Manning, 1994). In the same location as the PC section, Capelli et al. (2018) measured high concentrations in V, Ni, Fe, Cu, Zn and S that tend to peak in the intervals with the highest GR and U/Th. In the PC section, these intervals (highlighted as U/Th > 1.4) tend to coincide with the inflection points (minimum values) between the large-scale increasing-decreasing cycles in $\delta^{13}C_{carb}$ values and with transgressive or maximum flooding positions in the sequences. This suggests that the most negative $\delta^{13}C_{carb}$ values might represent lowest oxygen levels, highest availability of deposited organic matter for uranium fixation (Adams and Weaver, 1958; Jones and Manning, 1994; Zhao et al., 2016), highest precipitation of authigenic carbonate incorporating U in its structure (Zhao et al., 2016) and/or very low sedimentation rates (Algeo and Maynard, 2004).

The major trends in $\delta^{13}C_{carb}$ values, represented by the large-scale increasing-decreasing cycles in PC section, tend to be preserved in the relatively proximal setting of MDC section, at least for sequences 1 and 2 (Fig. 2). A similar increasing trend in the first large-scale cycle in $\delta^{13}C_{carb}$ values also occurs in MDC. The minimum $\delta^{13}C_{carb}$ values, although lower in the basin (avg. -8 to −6‰ in PC section) than in the relatively more proximal setting (avg. -6 to −4‰ in MDC section), coincide in both sites with the most organic-rich interval, the highest amount of ash layers, a relative increase in the occurrence of concretional levels within the fissile clastic mudstones, U-driven peaks in the GR profile (highest U/Th), and a transgressive position in the sequence. A similar trend is registered in subsurface wells on the Neuquén embayment (Hernandez Bilbao, 2016), which represent an analogous near-slope setting (Fig. 1A). The highest $\delta^{13}C_{carb}$ values also occur in intervals with relatively higher carbonate content, such as those described in the subsurface by Hernandez Bilbao (2016) or the Los Catutos Member in outcrops (Scasso et al., 2005). In addition, the major trend of the first large-scale cycle in $\delta^{13}C_{carb}$ values is also preserved in other basinal settings both in subsurface wells ~90 km southeast of the PC section (Morettini et al., 2015) and outcrops ~25 km north of the PC section (Weger et al., 2022). These basinal successions also display comparable trends to those of the PC section in the 2nd and 3rd increasing-decreasing cycles as well (Morettini et al., 2015; Weger et al., 2022).

Based on the evidence above, we propose that the large-scale cycles in $\delta^{13}C_{carb}$ values might reflect variations in oxygen conditions of the basinal waters, with the least-oxygen (anoxic to euxinic) episodes recording minimum $\delta^{13}C_{carb}$ values due to enhanced precipitation of authigenic carbonate. The minimum spikes in $\delta^{13}C_{carb}$ values are immediately followed by positive excursions that tend to coincide with large-scale transgressive to maximum flooding periods, thus suggesting sequence-stratigraphic control on the carbonate isotope variations. Although absolute $\delta^{13}C_{carb}$ values change laterally (Section 4.3), the fact that the major trends are preserved in successions of the Vaca Muerta Formation in different sites of the basin suggests that the large-scale trends in $\delta^{13}C_{carb}$ values might be driven by changes in the $\delta^{13}C_{DIC}$ of the bottom waters, thus producing synchronous major variations in slope and basin settings. Deposition in these settings probably took place most of the times in the oxygen deficient layer, given the facies and geochemical character of the laminated organic-rich mudstones. Evidence of periodic modifications in the position of the chemocline or mixing with more-oxygenated waters is given by the presence of bioturbation at cycle tops (Fig. 7). The changes in the oxygenation state of the basin might have been modulated by relative sea-level variations, with the transgressive portions of cycles recording the expansion of anoxic conditions towards basin margins, enhanced organic matter accumulation and increased chances of organic carbon recrystallization, thus yielding isotopically lighter authigenic carbonate (Figs. 3 and 7). Conversely, the regressive portions of the cycles would be recording a change towards dysoxic conditions, decreased organic matter accumulation and recrystallization, and yielding isotopically heavier authigenic carbonate (Figs. 3 and 7).

5.4. Proximal-distal variations in the $\delta^{13}C_{carb}$ values

The lateral change of the $\delta^{13}C_{carb}$ values such as seen in Fig. 5 (Section 4.3) can be best explained as a mixing signal between relative positive carbonate material exported from platforms and reflecting carbonate precipitated in approximate isotopic equilibrium with oceanic dissolved inorganic carbon, and authigenic carbonates formed on the sea floor (Fig. 7). As the platform gradually prograded into the basin or a reduction in the precipitation of authigenic carbonate occurred, the signal changed towards more positive values which were more reflective of the shallow water carbonate and perhaps reflective of the oceanic signal. This is similar to the mixing mechanism proposed for the Bahamas and other carbonate platforms (Swart and Eberli, 2005; Swart, 2008), with the exception that in this case one end member is mainly authigenic. However, in the case of the Neuquén Basin the basinal endmember would have been altered as it sank into the anoxic bottom water, and would have been dissolved-reprecipitated on the sea floor or within the pore space (Catalano et al., 2018; Milliken et al., 2019), producing carbonate material with isotopically negative $\delta^{13}C_{carb}$ values. Evidence of this mixing process was provided by Lanz et al. (2021) in a basinal site ~25 km north of the PC section. These authors analyzed wackestone-packstone beds from the lower ~100 m of the Vaca Muerta Formation, and found micrite with $\delta^{13}C_{carb}$ values both between 0 and + 2‰ (which they interpreted as precipitated in tropical warm shallow-water conditions) and between −8 and 0‰ (which they interpreted as precipitated near the sediment-water interface or during early diagenesis in reducing conditions and affected by organic matter alteration). These two endmembers (surface-derived vs. altered by organic-matter remineralization) are combined in our bulk rock measurements producing the observed mixing trend in $\delta^{13}C_{carb}$ values (Fig. 5).

The process of carbonate-mud export from carbonate shelves (shedding) is known to produce more significant effects near platforms and during highstands when carbonate production on the shelf is high (Schlager et al., 1994). Evidence for highstand shedding in the Vaca Muerta Formation is provided by 1) a basinward decrease in carbonate and skeletal content, and 2) an upward increase in carbonate and skeletal content within cycles, cycle sets and sequences (Rodriguez Blanco, 2016; Rodriguez Blanco et al., 2020; Figs. 3-4). Although productivity is probably a first-order control on TOC, the highstand shedding process

results in dilution of organic matter and lower TOC values in periplatform settings. In this environment, the highstand shedding process also results in heavier $\delta^{13}C_{carb}$ values, which are more influenced by shelf-derived carbonate material with surface-water isotopic compositions.

6. Conclusions

The $\delta^{13}C_{carb}$ values of the Vaca Muerta Formation show that two major processes acting in different parts of the system combine to control the measured $\delta^{13}C_{carb}$ values: 1) organic-matter alteration in poorly-oxygenated to anoxic basinal bottom waters with concomitant dissolution of biogenic carbonate and precipitation of authigenic carbonate (more negative values), and 2) shedding of platform-derived carbonate mud to the basin (more positive values). The relative influence of these processes controls the resultant $\delta^{13}C_{carb}$ values both in space and time. Positive shallow-water values on one end and negative organic-rich-influenced basinal values on the other result in mixed signatures along a proximal-distal trend. The carbonate-platform shedding process is recorded in two types of behavior that depend on the relative distance to the carbonate source: a basinward reduction in carbonate and skeletal contents, and a variable degree of organic-matter dilution. The higher sediment production on platforms during highstands and the concomitant increase of shedding are expressed in sequence-stratigraphic cycles as more carbonate-rich tops and more positive $\delta^{13}C_{carb}$ values that are more influenced by surface water values than by alteration of the organic matter.

Large-scale variations of basinal $\delta^{13}C_{carb}$ values might reflect changes in the accumulation of organic matter and the resultant isotopic composition of the water from which carbonates precipitate. Negative spikes followed by positive excursions record moments of lowest oxygen levels and/or highest availability of deposited organic matter for uranium fixation and/or highest precipitation of authigenic carbonate incorporating U in its structure and/or very low sedimentation rates. Isotopic variations are controlled by the sequence-stratigraphic framework, as minimum spikes immediately followed by positive excursions correspond to large-scale transgressive to maximum flooding periods. Although with different absolute values, major trends in $\delta^{13}C_{carb}$ values are similar in basinal and periplatform settings suggesting that changes in the $\delta^{13}C_{DIC}$ values of the bottom waters, probably controlled by relative sea level, might have produced synchronous major variations in different sites of the basin. Hence, carbonate isotope ($\delta^{13}C_{carb}$) stratigraphy might be a useful tool to refine correlations within the Vaca Muerta Formation. The $\delta^{13}C_{carb}$ values of the Neuquén Basin are more negative than in the Tethyan Tithonian-Berriasian profile, indicating the influence of local processes on the $\delta^{13}C_{carb}$ signal and the near complete obliteration of the global carbon cycling during this time period. This strong local control implies that caution should be taken when relating $\delta^{13}C_{carb}$ profiles from epicontinental seas to the global carbon cycle in deep time.

Data availability

Datasets related to this article can be found at http://dx.doi.org/...., an open-source online data repository hosted at Mendeley Data.

CRediT authorship contribution statement

Leticia Rodriguez Blanco: Conceptualization, Methodology, Formal analysis, Investigation, Writing – original draft, Writing – review & editing, Visualization, Project administration. **Peter K. Swart:** Conceptualization, Methodology, Validation, Resources, Writing – review & editing, Funding acquisition. **Gregor P. Eberli:** Conceptualization, Resources, Writing – review & editing, Supervision, Funding acquisition. **Ralf J. Weger:** Resources, Writing – review & editing, Funding acquisition.

Declaration of Competing Interest

The authors declare that they have no known competing financial interests or personal relationships that could have appeared to influence the work reported in this paper.

Data availability

Data is in the Supplementary Data file

Acknowledgements

The project was funded by the CSL – Center for Carbonate Research with financial support from its industrial associates. L. Rodriguez Blanco acknowledges a Fulbright fellowship for partial support of this study. Stable isotope and organic carbon analyses were measured in the Stable Isotope Laboratory of the University of Miami, and Amel Saied and Chris Keiser are thanked for technical help. We also thank Max Tenaglia, Laura Rueda and Donald F. McNeill for collaboration in fieldwork and sample processing. Editor Shucheng Xie, M.S. Fantle and two anonymous reviewers are thanked for their comments, which greatly helped to improve the manuscript.

Appendix A. Supplementary data

Supplementary data to this article can be found online at https://doi.org/10.1016/j.palaeo.2022.111208.

References

Adams, J.A., Weaver, C.E., 1958. Thorium-to-uranium ratios as indicators of sedimentary processes: example of concept of geochemical facies. AAPG Bull. 42 (2), 387–430.
Afsar, F., 2010. Einfluss petrographischer Merkmale auf akustische Geschwindigkeiten in gemischt siliziklastisch-karbonatischen Gesteinen (Picún Leufú-Formation, Neuquén Becken, Argentinien). Master-Thesis. Universität Bremen.
Aguirre Urreta, M.B., Vennari, V.V., 2013. Amonites y bioestratigrafía de la Formación Vaca Muerta en tres pozos de El Trapial. Chevron internal report.
Aguirre Urreta, M.B., Price, G.D., Ruffell, A.H., Lazo, D.G., Kalin, R.M., Ogle, N., Rawson, P.F., 2008. Southern Hemisphere early cretaceous (Valanginian-early Barremian) carbon and oxygen isotope curves from the Neuquén Basin, Argentina. Cretac. Res. 29, 87–99.
Aguirre Urreta, M.B., Vennari, V.V., Lescano, M., Naipauer, M., Concheyro, A., Ramos, V. A., 2014. Bioestratigrafía y Geocronología de Alta Resolución de la Formación Vaca Muerta, Cuenca Neuquina. In: IX Congreso de Exploración y Desarrollo de Hidrocarburos. Mendoza. Trabajos Técnicos, vol. 2, pp. 245–268.
Ahm, A.-S.C., Husson, J., 2022. Local and Global Controls on Carbon Isotope Chemostratigraphy. (Elements in Geochemical Tracers in Earth System Science). Cambridge University Press, Cambridge. https://doi.org/10.1017/9781009028882.
Algeo, T.J., Maynard, J.B., 2004. Trace-element behavior and redox facies in core shales of Upper Pennsylvanian Kansas-type cyclothems. Chem. Geol. 206, 289–318.
Allan, J.R., Matthews, R.K., 1982. Isotope signatures associated with early meteoric diagenesis. Sedimentology 29, 797–817.
Bodin, S., Fiet, N., Godet, A., Matera, V., Westermann, S., Clément, A., Janssen, N.M.M., Stille, P., Föllmi, K.B., 2009. Early cretaceous (late Berriasian to early Aptian) palaeoceanographic change along the northwestern Tethyan margin (Vocontian Trough, southeastern France): δ13C, δ18O and Sr-isotope belemnite and whole-rock records. Cretac. Res. 30, 1247–1462.
Brisson, I.E., Fasola, M.E., Villar, H.J., 2020. Organic geochemical patterns of the Vaca Muerta Formation. In: Minisini, D., Fantín, M., Lanusse Noguera, I., Leanza, H. (Eds.), Integrated Geology of Unconventionals: The Case of the Vaca Muerta Play, Argentina. AAPG Memoir, vol. 121, pp. 297–328.
Capelli, I.A., Scasso, R.A., Kietzmann, D.A., Cravero, F., Minisini, D., Catalano, J.P., 2018. Mineralogical and geochemical trends of the Vaca Muerta-Quintuco system in the Puerta Curaco section, Neuquén Basin. Rev. Asoc. Geol. Argent. 75, 210–228.
Capelli, I.A., Scasso, R.A., Cravero, F., Kietzmann, D.A., Vallejo, D., Adatte, T., 2021a. Late-diagenetic clay mineral assemblages in carbonatized ash beds of the Vaca Muerta Formation (Neuquén Basin, Argentina): Insights into the diagenetic formation of chlorite. Mar. Pet. Geol. 132, 105207.
Capelli, I.A., Scasso, R.A., Spangenberg, J., Kietzmann, D., Cravero, F., Duperron, M., Adatte, T., 2021b. Mineralogy and geochemistry of deeply-buried marine sediments of the Vaca Muerta-Quintuco system in the Neuquén Basin (Chacay Melehue section), Argentina: paleoclimatic and paleoenvironmental implications for the global Tithonian-Valanginian reconstructions. J. S. Am. Earth Sci. 107, 103103.
Catalano, J.P., Scasso, R.A., Kietzmann, D., Föllmi, K., Spangenberg, J., Capelli, I., 2018. Carbonate sedimentology and diagenesis of the Vaca Muerta Formation at Puerta Curaco, Neuquén Basin, Argentina. In: 10° Congreso de Exploración y Desarrollo de Hidrocarburos. Simposio de Recursos No Convencionales, pp. 481–501.

Christ, N., Immenhauser, A., Amour, F., Mutti, M., Preston, R., Whitaker, F.F., Peterhaensel, A., Egenhoff, S.O., Dunn, P.A., Agar, S.M., 2012. Triassic Latemar cycle tops - Subaerial exposure of platform carbonates under tropical arid climate. Sediment. Geol. 265, 1–29.
Coleman, M.L., Raiswell, R., 1981. Carbon, oxygen and sulphur isotope variations in concretions from the Upper Lias of N.E. England. Geochem. Cosmochem. Acta 45, 329–340.
Cramer, B.D., Jarvis, I., 2020. Carbon isotope stratigraphy. In: Gradstein, F.M., Ogg, J.G., Schmitz, M.D., Ogg, G.M. (Eds.), Geologic Time Scale 2020. Elsevier, pp. 309–343.
Domínguez, R.F., Reijenstein, H., Kohler, G., Sattler, F., Moreno, M.J., Gómez Rivarola, L., Borgnia, M., 2017. Distribución regional de quiebres de clinoformas del sistema Vaca Muerta-Quintuco. In: XX Congreso Geológico Argentino, Tucumán, Argentina. Actas Simposio Geología de la Formación Vaca Muerta, pp. 38–45.
Domínguez, R.F., Catuneanu, O., Reijenstein, H.M., Notta, R., Posamentier, H.W., 2020. Sequence stratigraphy and the three-dimensional distribution of organic-rich units. In: Minisini, D., Fantín, M., Lanusse Noguera, I., Leanza, H. (Eds.), Integrated Geology of Unconventionals: The Case of the Vaca Muerta Play, Argentina. AAPG Memoir, vol. 121, pp. 163–200.
Doyle, P., Poire, D.G., Spalletti, L.A., Pirrie, D., Brenchley, P., Matheos, S.D., Veiga, G.D., Spalletti, L.A., 2005. Relative oxygenation of the Tithonian – Valanginian Vaca Muerta-Chachao formations of the Mendoza Shelf, Neuquén Basin, Argentina. In: Howell, J.A., Schwarz, E. (Eds.), The Neuquén Basin, Argentina: A Case Study in Sequence Stratigraphy and Basin Dynamics, Geological Society, London, Special Publications, vol. 252, pp. 185–206.
Erba, E., Bartolini, A., Larson, R.L., 2004. Valanginian Weissert ocean anoxic event. Geology 32, 149–152.
Föllmi, K.B., 2012. Early cretaceous life, climate and anoxia. Cretac. Res. 35, 230–257.
Föllmi, K.B., Weissert, H., Bisping, M., Funk, H., 1994. Phosphogenesis, carbon-isotope stratigraphy, and carbonate-platform evolution along the lower cretaceous northern Tethyan margin. Geol. Soc. Am. Bull. 106, 729–746.
Franzese, J.R., Spalletti, L.A., 2001. Late Triassic-early Jurassic continental extension in southwestern Gondwana: tectonic segmentation and pre-break-up rifting. J. S. Am. Earth Sci. 14, 257–270.
Gale, A.S., Mutterlose, J., Batenburg, S., Gradstein, F.M., Agterberg, F.P., Ogg, J.G., Petrizzo, M.R., 2020. The cretaceous period. In: Gradstein, F.M., Ogg, J.G., Schmitz, M.D., Ogg, G.M. (Eds.), Geologic Time Scale 2020. Elsevier, pp. 1023–1086.
Gasparini, Z., Spalletti, L., De La Fuente, M., 1997. Tithonian Marine Reptiles of the Western Neuquén Basin, Argentina. Facies Palaeoenviron. Geobios 30, 701–712.
Gasparini, Z., Fernandez, M.S., De La Fuente, M., Herrera, Y., Codorniu, L., Garrido, A., 2015. Reptiles from lithographic limestones of the Los Catutos Member (Middle-Upper Tithonian), Neuquen Province, Argentina: an essay onits taxonomic composition and preservation in an environmental and geographic context. Ameghiniana 52, 1–28.
Grabowski, J., Bakhmutov, V., Kdýr, Š., Krobicki, M., Pruner, P., Reháková, D., Schnabl, P., Stoykova, K., Wierzbowski, H., 2019. Integrated stratigraphy and palaeoenvironmental interpretation of the Upper Kimmeridgian to Lower Berriasian pelagic sequences of the Velykyi Kamianets section (Pieniny Klippen Belt, Ukraine). Palaeogeogr. Palaeoclimatol. Palaeoecol. 532, 109216.
Hallam, A., 1983. Early and midJurassic molluscan biogeography and the establishment of the Central Atlantic Seaway. Palaeogeogr. Palaeoclimatol. Palaeoecol. 43, 181–193.
Hernandez Bilbao, E., 2016. High-Resolution Chemostratigraphy, Sequence Stratigraphic Correlation, Porosity and Fracture Characterization of the Vaca Muerta Formation, Neuquén Basin, Argentina, vol. 221. Colorado School of Mines. Dissertation. 10113602.
Hesselbo, S.P., Ogg, J.G., Ruhl, M., Hinnov, L.A., Huang, C.J., 2020. The Jurassic Period. In: Gradstein, F.M., Ogg, J.G., Schmitz, M.D., Ogg, G.M. (Eds.), Geologic Time Scale 2020. Elsevier, pp. 955–1021.
Hillebrandt, A., Westermann, G., Callomon, J., Detterman, R., 1993. Ammonites of the circum-Pacific region. In: Westermann, G. (Ed.), The Jurassic of the Circum-Pacific. Cambridge University Press, pp. 342–359. https://doi.org/10.1017/CBO9780511529375.026.
Howell, J.A., Schwarz, E., Spalletti, L.A., Veiga, G.D., 2005. The Neuquén Basin: An overview. In: Veiga, G.D., et al. (Eds.), The Neuquén Basin, Argentina: A Case Study in Sequence Stratigraphy and Basin Dynamics, Geol. Soc. London Spec. Publ, vol. 252, pp. 1–14.
Jenkyns, H.C., Clayton, C.J., 1997. Lower Jurassic epicontinental carbonates and mudstones from England and Wales: chemostratigraphic signals and the early Toarcian event. Sedimentology 44, 687–706.
Jones, B., Manning, D.A.C., 1994. Comparison of geochemical indices used for the interpretation of palaeoredox conditions in ancient mudstones. Chem. Geol. 111, 111–129.
Katz, M.E., Wright, T., Miller, K.G., Cramer, B.S., Fennel, K., Falkowski, P.G., 2005. Biological overprint of the geological carbon cycle. Mar. Geol. 217, 323–338.
Kietzmann, D.A., Martín-Chivelet, D.A.J., Palma, R.M., López-Gómez, J., Lescano, M., Concheyro, A., 2011. Evidence of precessional and eccentricity orbital cycles in a Tithonian source rock: the mid-outer carbonate ramp of the Vaca Muerta Formation, northern Neuquén Basin, Argentina. AAPG Bull. 95, 1459–1474. https://doi.org/10.1306/01271110084.
Kietzmann, D.A., Ambrosio, A.L., Suriano, J., Alonso, S., Vennari, V.V., Aguirre-Urreta, M.B., Depine, G., Repol, D., 2014. Variaciones de facies de las secuencias basales de la Formación Vaca Muerta en su localidad tipo (Sierra de la Vaca Muerta), cuenca Neuquina. In: IX Congreso de Exploración y Desarrollo de Hidrocarburos, Mendoza. Trabajos Técnicos, vol. 2, pp. 299–317.
Krim, N., Bonnel, C., Tribovillard, N., Imbert, P., Aubourg, C., Riboulleau, A., Bout-Roumazeilles, V., Hoareau, G., Fasentieux, B., 2017. Paleoenvironmental evolution of the southern Neuquèn basin (Argentina) during the Tithonian-Berriasian (Vaca Muerta and Picún Leufú Formations): a multi-proxy approach. Bull. Soc. Géol. France 188. https://doi.org/10.1051/bsgf/2017196, 34 pp.
Krim, N., Tribovillard, N., Riboulleau, A., Bout-Roumazeilles, V., Bonnel, C., Imbert, P., Aubourg, C., Hoareau, G., Fasentieux, B., 2019. Reconstruction of palaeoenvironmental conditions of the Vaca Muerta formation in the southern part of the Neuquén Basin (Tithonian-Valanginian): Evidences of initial short-lived development of anoxia. Mar. Pet. Geol. 103, 176–201.
Kump, L.R., Arthur, M.A., 1999. Interpreting carbon-isotope excursions: carbonates and organic Matter. Chem. Geol. 161, 181–198.
Lanz, M.R., Azmy, K., Cesaretti, N.N., Fortunatti, N.B., 2021. Diagenesis of the Vaca Muerta Formation, Neuquén Basin: evidence from petrography, microthermometry and geochemistry. Mar. Pet. Geol. 124, 104769.
Leanza, H.A., 1973. Estudio sobre los cambios faciales de los estratos limítrofes Jurásico-Cretácicos entre Loncopué y Picún Leufú, provincia de Neuquén, República Argentina. In: Revista de la Asociación Geológica Argentina XXVIII, 2, pp. 97–132.
Leanza, H.A., Zeiss, A., 1990. Upper Jurassic lithographic limestones from Argentina (Neuquén Basin): stratigraphy and fossils. Facies 22, 169–186.
Leanza, H.A., Kietzmann, D.A., Iglesia Llanos, M.P., Kohan Martínez, M., 2020. Stratigraphic context: cyclostratigraphy, magnetostratigraphy, and seismic stratigraphy. In: Minisini, D., Fantín, M., Lanusse Noguera, I., Leanza, H. (Eds.), Integrated Geology of Unconventionals: The Case of the Vaca Muerta Play, Argentina, AAPG Memoir, vol. 121, pp. 39–60.
Legarreta, L., Uliana, M.A., 1991. Jurassic-cretaceous marine oscillations and geometry of back-arc basin fill, central argentine Andes. In: Macdonald, D.I. (Ed.), Sedimentation, Tectonics and Eustacy, Spec. Publ. Int. Assoc. Sed, vol. 12, pp. 429–450.
Legarreta, L., Uliana, M.A., 1996. The Jurassic succession in west-Central Argentina: stratal patterns, sequences and paleogeographic evolution. Palaeogeogr. Palaeoclimatol. Palaeoecol. 120, 303–330.
Legarreta, L., Villar, H.J., 2015. The Vaca Muerta Formation (Late Jurassic - Early Cretaceous), Neuquén Basin, Argentina: Sequences, Facies and Source Rock Characteristics. URTeC: 2170906.
Lini, A., Weissert, H., Erba, E., 1992. The Valanginian carbon isotope event: a first episode of greenhouse climate conditions during the cretaceous. Terra Nova 4, 374–384.
Lohmann, K.C., 1988. Geochemical patterns of meteoric diagenetic systems and their application to studies of paleokarst. In: James, N.P., Choquette, P.W. (Eds.), Paleokarst. Springer, New York, NY. https://doi.org/10.1007/978-1-4612-3748-8_3.
Massaferro, J.L., Zeller, M., Giunta, D.L., Sagasti, G., Eberli, G.P., 2014. Evolución del sistema mixto Tithoniano-Valanginiano (formaciones Vaca Muerta, Quintuco y equivalentes) a partir de estudios de afloramientos y subsuelo, centro-sur de la Cuenca Neuquina. In: Proceedings IX Congreso Exploración y Desarrollo de Hidrocarburos: Simposio Recursos No Convencionales, Mendoza, Argentina, pp. 251–274.
McNeill, D.F., Swart, P., Rodriguez Blanco, L., Tenaglia, M., Weger, R.J., Rueda Sanchez, L.E., Burke, B.G., Klaus, J.S., Eberli, G.P., 2016. Concretions in the Mixed System: Microbial-Driven Early Marine Calcite Cementation. AAPG Search and Discovery Article 90259. AAPG Annual Convention and Exhibition, Calgary, Canada.
Meissinger, V., Lo Forte, G., 2014. El shale desde el punto de vista diagenético: el aporte volcánico en la diagénesis temprana de la Formación Vaca Muerta. In: IX Congreso de Exploración y Desarrollo de Hidrocarburos, Mendoza. Trabajos Técnicos, 1, pp. 403–426.
Milliken, K.L., Reeda, R.M., McCarty, D.K., Bishop, J., Lipinski, C.J., Fischer, T.B., Crousse, L., Reijenstein, H., 2019. Grain assemblages and diagenesis in the Vaca Muerta Formation (Jurassic-Cretaceous), Neuquén Basin, Argentina. Sediment. Geol. 380, 45–64.
Minisini, D., Fantín, M., Lanusse Noguera, I., Leanza, H.A., 2020. Integrated Geology of Unconventionals: The Case of the Vaca Muerta Play, Argentina. In: AAPG Memoir 121.
Mitchum, R.M., Uliana, M.A., 1985. Seismic Stratigraphy of carbonate depositional sequences, Upper Jurassic-Lower Cretaceous, Neuquen Basin, Argentina. AAPG Mem. 39, 255–274.
Morettini, E., Godino, G., Smith, L.B., Massaferro, J.L., 2015. The Vaca Muerta-Quintuco Mixed Depositional System: New Insights from Carbon Stable Isotopes (δ^{13}Ccarb and δ^{13}Corg) and Geochemical Data at the Jurassic-Cretaceous Boundary (Neuquén Basin, West Argentina). In: AAPG Search and Discovery Article 90216. AAPG Annual Convention and Exhibition, Denver, CO.
Otharán, G., 2020. Sedimentología y análisis de facies de la Formación Vaca Muerta (Tithoniano-Valanginiano), Cuenca Neuquina. El rol de los flujos de fango en la depositación de espesas sucesiones de lutitas. Tesis doctoral. https://doi.org/10.13140/RG.2.2.32858.67520/1.
Otharán, G., Zavala, C., Arcuri, M., Di Meglio, M., Zorzano, A., Marchal, D., Köhler, G., 2020. Facies analysis of fine-grained deposits related to muddy underflows. Vaca Muerta Formation (Tithonian-Valanginian), central Neuquen Basin, Argentina. Andean Geol. 47, 384–417. https://doi.org/10.5027/andgeoV47n2-3061.
Parent, H., Garrido, A.C., Scherzinger, A., Schweigert, G., Fözy, I., 2015. The Tithonian-lower Valanginian stratigraphy and ammonite fauna of the Vaca Muerta Formation in Pampa Tril, Neuquén basin, Argentina. Boletin Inst. Fisiografia Geol. 86, 96 pp.
Paz, M., Ponce, J.J., Buatois, L.A., Mángano, M.G., Carmona, N.B., Pereira, E., Desjardins, P.R., 2019. Bottomset and foreset sedimentary processes in the mixed carbonate-siliciclastic Upper Jurassic-lower cretaceous Vaca Muerta Formation, Picún Leufú Area, Argentina. Sediment. Geol. 389, 161–185.
Raiswell, R., 1976. The microbiological formation of carbonate concretions in the Upper Lias of NE England. Chem. Geol. 18, 227–244.

Ramos, V.A., 2010. The tectonic regime along the Andes: present-day and Mesozoic regimes. Geol. J. 45, 2–25. https://doi.org/10.1002/gj.1193.
Ramos, V.A., Aleman, A., 2000. Tectonic evolution of the Andes. In: Cordani, U.G., Milani, E.J., Thomaz Filho, A., Campos, D.A. (Eds.), Tectonic Evolution of South America, 31st. International Geological Congress, Río de Janeiro, pp. 635–685.
Ramos, V.A., Naipauer, M., Leanza, H.A., Sigismondi, M.E., 2020. An exceptional tectonic setting along the Andean continental margin. In: Minisini, D., Fantín, M., Lanusse Noguera, I., Leanza, H. (Eds.), Integrated Geology of Unconventionals: The Case of the Vaca Muerta Play, Argentina, AAPG Memoir, vol. 121, pp. 25–38.
Reboulet, S., Szives, O., Aguirre-Urreta, B., Barragán, R., Company, M., Idakieva, V., Ivanov, M., Kakabadze, M.V., Moreno-Bedmar, J.A., Sandoval, J., Baraboshkin, E.J., Çağlar, M.K., Főzy, I., González-Arreola, C., Kenjo, S., Lukeneder, A., Raisossadat, S. N., Rawson, P.F., Tavera, J.M., 2014. Report on the 5th International meeting of the IUGS lower cretaceous Ammonite Working Group, the Kilian Group (Ankara, Turkey, 31st August 2013). Cretac. Res. 50, 126–137.
Reijenstein, H.M., Posamentier, H.W., Bande, A., Lozano, F.A., Domínguez, R.F., Wilson, R., Catuneanu, O., Galeazzi, S., 2020. Seismic geomorphology, depositional elements, and clinoform sedimentary processes: Impact on unconventional reservoir prediction. In: Minisini, D., Fantín, M., Lanusse Noguera, I., Leanza, H. (Eds.), Integrated Geology of Unconventionals: The Case of the Vaca Muerta Play, Argentina, AAPG Memoir, vol. 121, pp. 237–266.
Riccardi, A.C., 1991. Jurassic and cretaceous marine connections between the Southeast Pacific and Tethys. Palaeogeogr. Palaeoclimatol. Palaeoecol. 87, 155–189.
Rodriguez Blanco, L., 2016. Distribution and Source of Carbonate-Rich Intervals within the Vaca Muerta-Quintuco Mixed System, Neuquén Basin, Argentina. University of Miami, p. 622. Open Access Theses.
Rodriguez Blanco, L., Eberli, G.P., Weger, R.J., Swart, P., Tenaglia, M., Rueda, L., McNeill, D., 2020. A Periplatform Ooze within a mixed Siliciclastic-Carbonate System – Vaca Muerta Formation, Neuquén Basin. Sediment. Geol. 396, 105521 https://doi.org/10.1016/j.sedgeo.2019.105521.
Rodriguez Blanco, L., Eberli, G.P., Weger, R.J., McNeill, D., Swart, P., 2022. Quantifying concretion distribution in shales of the Vaca Muerta-Quintuco system, Neuquén Basin, Argentina. AAPG Bull. 106, 409–436. https://doi.org/10.1306/08182120059.
Rutman, P., Hoareau, G., Kluska, J.-M., Lejay, A., Fialips, C., Gelin, F., Aubourg, C., Hernandez Bilbao, E., 2021. Diagenesis and alteration of subsurface volcanic ash beds of the Vaca Muerta Formation, Argentina. Mar. Pet. Geol. 132, 105220.
Saltzman, M.R., Thomas, E., 2012. Carbon Isotope Stratigraphy. In: Gradstein, F.M., Ogg, J.G., Schmitz, M.D., Ogg, G.M. (Eds.), The Geologic Time Scale 2012. Elsevier, Oxford, pp. 207–232.
Scasso, R.A., Alonso, M.S., Lanes, S., Villar, H.J., Laffitte, G., 2005. Geochemistry and petrology of a Middle Tithonian limestone-marl rhythmite in the Neuquén Basin, Argentina: depositional and burial history. In: Veiga, G.D., Spalletti, L.A., Howell, J. A., Schwarz, E. (Eds.), The Neuquén Basin, Argentina: A Case Study in Sequence Stratigraphy and Basin Dynamics, Geological Society, London, Special Publications, vol. 252, pp. 207–229.
Schlager, W., Riejmer, J.J.G., Droxler, A., 1994. Highstand shedding of carbonate platforms. J. Sediment. Res. 64 (3), 270–281.
Scholle, P.A., Arthur, M.A., 1980. Carbon isotope fluctuations in Cretaceous Pelagic limestones: potential stratigraphic and petroleum exploration tool. AAPG Bull. 64, 67–87.
Schrag, D.P., Higgins, J.A., Macdonald, F.A., Johnston, D.T., 2013. Authigenic carbonate and the history of the global carbon cycle. Science 339 (6119), 540–543.
Spalletti, L.A., Franzese, J.R., Matheos, S.D., Schwarz, E., 2000. Sequence stratigraphy of a tidally dominated carbonate-siliciclastic ramp; the Tithonian-early Berriasian of the Southern Neuquén Basin, Argentina. J. Geol. Soc. Lond. 157, 433–446.
Spalletti, L.A., Schwarz, E., Veiga, G.D., 2014. Geoquímica inorgánica como indicador de procedencia y ambiente sedimentario en sucesiones de lutitas negras: los depósitos transgresivos titonianos (Formación Vaca Muerta) de la Cuenca Neuquina, Argentina. Andean Geol. 41 (2), 401–435.
Spalletti, L.A., Remírez, M.N., Sagasti, G., 2019. Geochemistry of aggradational - Progradational sequence sets of the Upper Jurassic – lower cretaceous Vaca Muerta shales (Añelo area, Neuquén Basin, Argentina): relation to changes in accommodation and marine anoxia. J. S. Am. Earth Sci. 93, 495–509.
Sun, X., Turchyn, A.V., 2014. Significant contribution of authigenic carbonate to marine carbon burial. Nat. Geosci. 7, 201–204.
Swart, P.K., 2008. Global synchronous changes in the carbon isotopic composition of carbonate sediments unrelated to changes in the global carbon cycle. Proc. Natl. Acad. Sci. 105, 13741–13745.
Swart, P.K., Eberli, G.P., 2005. The nature of the d^{13}C of periplatform sediments: implications for stratigraphy and the global carbon cycle. Sediment. Geol. 175, 115–130.
Swart, P.K., Burns, S.J., Leder, J.J., 1991. Fractionation of the stable isotopes of oxygen and carbon in carbon dioxide during the reaction of calcite with phosphoric acid as a function of temperature and technique. Chem. Geol. 86, 89–96.
Uliana, M.A., Biddle, K.T., Cerdan, J., 1995. Mesozoic extension and the formation of Argentina sedimentary basins. In: Tankard, A.J., Balkwill, H.R. (Eds.), Extensional Tectonics and Stratigraphy of the North Atlantic Margins. https://doi.org/10.1306/M46497C39.
Veizer, J., Holser, W.T., Wilgus, C.K., 1980. Correlation of $^{13}C/^{12}C$ and $^{34}S/^{32}S$ secular variations. Geochim. Cosmochim. Acta 44, 579–587.
Vergani, G.D., Tankard, A., Belotti, H.J., Welsink, H.J., 1995. Tectonic evolution and paleogeography of the Neuquén Basin, Argentina. In: Tankard, A.J., et al. (Eds.), Petroleum Basins of South America, AAPG Memoir, vol. 62, pp. 383–402.
Weger, R.J., Murray, S.T., McNeill, D.F., Swart, P.K., Eberli, G.P., Rodriguez Blanco, L., Tenaglia, M., Rueda, L.E., 2019. Paleothermometry and distribution of calcite beef in the Vaca Muerta Formation, Neuquen Basin, Argentina. AAPG Bull. 103 (4), 631–650.
Weger, R.J., Eberli, G.P., Rodriguez Blanco, L., Tenaglia, M., Swart, P.K., 2022. Finding a VOICE in the Southern Hemisphere: A new record of global organic carbon? GSA Bull.
Weissert, H., Erba, E., 2004. Volcanism, CO2 and palaeoclimate: a Late Jurassic–Early Cretaceous carbon and oxygen isotope record. J. Geol. Soc. Lond. 161, 1–8.
Wendler, I., 2013. A critical evaluation of carbon isotope stratigraphy and biostratigraphic implications for late cretaceous global correlation. Earth Sci. Rev. 126, 116–146. https://doi.org/10.1016/j.earscirev.2013.08.003.
Zeller, M., 2013. Facies, Geometries and Sequence Stratigraphy of the Mixed Carbonate-Siliciclastic Quintuco-Vaca Muerta System in the Neuquén Basin, Argentina: An Integrated Approach. University of Miami. Open Access Dissertations. Paper 1099.
Zeller, M., Verwer, K., Eberli, G.P., Massaferro, J.L., Schwarz, E., Spalletti, L.A., 2015. Depositional controls on mixed carbonate-siliciclastic cycles and sequences on gently inclined shelf profiles. Sedimentology 62 (7), 2009–2037.
Zhao, M.-Y., Zheng, Y.-F., Zhao, Y.-Y., 2016. Seeking a geochemical identifier for authigenic carbonate. Nat. Commun. 7, 10885.